ADVANCED ENERGY MATERIALS
www.advenergymat.de

Asymmetric Nonfullerene Small Molecule Acceptors for Organic Solar Cells

*Chao Li, Huiting Fu, Tian Xia, and Yanming Sun**

Symmetry breaking provides a new material design strategy for nonfullerene small molecule acceptors (SMAs). The past 10 years have witnessed significant advances in asymmetric nonfullerene SMAs in organic solar cells (OSCs) with power conversion efficiency (PCE) increasing from ≈1% to ≈14%. In this review, the progress of asymmetric nonfullerene SMAs, including early reports of asymmetric nonfullerene SMAs, asymmetric PDI-based nonfullerene SMAs, and asymmetric acceptor–donor–acceptor (A–D–A)-type nonfullerene SMAs, is summarized. The structure–property relationships and the perspectives for future development of asymmetric nonfullerene SMAs are also discussed.

1. Introduction

As one of the promising photovoltaic technologies for converting solar energy into electricity, organic solar cells (OSCs) have received a great deal of attention because of their advantages, including mechanic flexibility, light weight, solution processibility, and semitransparency.[1–5] State-of-the-art OSCs are usually fabricated with a bulk-heterojunction structure comprising a blend of a polymer donor and a small molecule acceptor (SMA), in which SMA can be categorized into symmetric SMA and asymmetric SMA according to their molecular symmetry. Thanks to the molecular asymmetric structure of the widely used phenyl-C_{61}-butyric acid methyl ester ($PC_{61}BM$) and phenyl-C_{71}-butyric acid methyl ester ($PC_{71}BM$), asymmetric fullerene SMAs had been associated with the rise and development of OSCs in the past decades.[6–11] However, the application of asymmetric fullerene SMAs was limited to a great extent owing to their disadvantages, such as restricted structure modification, weak absorption in the visible region, high production costs, and morphological instability. Therefore, nonfullerene SMAs have caught great research interest, and recent years have seen the rapid development and tremendous progress of both symmetric nonfullerene SMAs and asymmetric nonfullerene SMAs.[12–38]

In fact, the development of asymmetric nonfullerene SMAs could be traced back to 2010, in which Meredith's group[30] and Anthony's group[31] reported asymmetric K12 and asymmetric EDPD acceptors, respectively. Since then, several promising asymmetric nonfullerene SMAs have been developed to pair with the polymer donor P3HT.[39–43] However, the development of asymmetric nonfullerene SMAs remained nearly stagnant from 2015 to 2016. This unfavorable situation has changed when asymmetric nonfullerene SMAs began to emerge in 2017 and experienced rapid development in the past 3 years.[32–37] In addition to maintaining the advantages of symmetric nonfullerene SMAs,[12–29] such as chemical structure diversity and good adjustability in photoelectrical properties, asymmetric nonfullerene SMAs may additionally exhibit stronger intermolecular binding energy and larger dipole moment than symmetric nonfullerene SMA counterparts.[33,35,44] Both stronger intermolecular binding energy and larger dipole moment are beneficial to reinforce intermolecular interaction, rendering asymmetric nonfullerene SMAs a promising class of nonfullerene SMAs to increase the fill factor (FF) and power conversion efficiency (PCE) in OSCs. To date, the PCEs of OSCs based on asymmetric nonfullerene SMAs have gradually increased from 1.27% in 2010 to nearly 14% in 2019.[31,38]

There have been a large number of review articles summarizing the recent development of symmetric nonfullerene SMAs.[13–18,45–51] However, to the best of our knowledge, there has been no one review article specially focusing on asymmetric nonfullerene SMAs so far. Given the significant progress achieved recently for asymmetric nonfullerene SMAs, it is timely to briefly review the development of asymmetric nonfullerene SMAs in the past decade. Here, we first summarize the recent advances of asymmetric nonfullerene SMAs, including early reports of asymmetric nonfullerene SMAs, asymmetric PDI-based nonfullerene SMAs, and asymmetric acceptor–donor–acceptor (A–D–A)-type nonfullerene SMAs. Finally, we discuss the structure–property relationships and the perspectives for future development of asymmetric nonfullerene SMAs.

2. Early Reports of Asymmetric Nonfullerene SMAs

In view of the shortcomings of asymmetric fullerene SMAs, some attempts have been made to develop asymmetric nonfullerene SMAs with easy access, tunable optical/electrochemical properties, and wide possibility of functionalization.[39–43] Generally, these asymmetric nonfullerene SMAs could be

C. Li, H. Fu, T. Xia, Prof. Y. Sun
School of Chemistry
Beihang University
Beijing 100191, China
E-mail: sunym@buaa.edu.cn

The ORCID identification number(s) for the author(s) of this article can be found under https://doi.org/10.1002/aenm.201900999.

DOI: 10.1002/aenm.201900999

rationally designed through the strategy of introducing a strongly electron-withdrawing group onto symmetric core. For example, early in 2010, an asymmetric nonfullerene SMA named K12 was reported by Meredith and co-workers,[30] which comprises a dicyanovinyl-substituted benzothiadiazole group and fluorene core (**Figure 1**). K12 can serve as a nonfullerene SMA to blend with polymer donor P3HT. A PCE of 0.73% was achieved, and the PCE was further promoted to 1.43% when the symmetric dithienosilole core was employed (**Table 1**).[39] Meanwhile, Anthony and co-workers[31] reported an asymmetric nonfullerene SMA named EDPD by incorporating a cyano group into the symmetric silylethyne-substituted pentacene core. The EDPD possessed a lowest unoccupied molecular orbital (LUMO) energy level of −3.50 eV. When paired with P3HT, a higher open-circuit voltage (V_{oc}) of 0.84 V was achieved. However, mainly due to the low short-circuit current density (J_{sc}) and FF, EDPD-based OSCs only delivered a PCE of 1.29%. In 2012, when a cyano group was used to modify the fluoranthene-fused imide (FFI) core, Pei and co-workers[40] synthesized an asymmetric nonfullerene acceptor named FFI-1, which exhibited a low PCE of 1.86% in OSCs. Later, the PCE was improved to over 2% when the thiophenyl groups or cyano substituent in FFI-1 were chemically modified.[41,42] In 2014, through the introduction of an electron-withdrawing n-hexyl-naphthalimide moiety to the C_5-symmetric corannulene core, Cao and co-workers[43] developed an asymmetric nonfullerene SMA named Cor-NI. A PCE of 1.03% was obtained for OSCs based on P3HT:Cor-NI blend. The aforementioned results demonstrated that incorporation of a strongly electron-withdrawing group into symmetric core was an effective method to design asymmetric nonfullerene SMAs. With appropriate LUMO energy levels driven by the electron-withdrawing groups, these asymmetric nonfullerene SMAs performed well with P3HT. Compared with PCBM, these asymmetric nonfullerene SMAs exhibited a higher LUMO energy level, which was beneficial for obtaining a higher V_{oc} in the corresponding OSC devices. However, mainly due to the very limited complementary absorptions between these asymmetric nonfullerene SMAs and P3HT as well as unfavorable blend morphology, these asymmetric nonfullerene SMA-based devices often suffered from relatively J_{sc} and FF, which resulted in an overall low PCEs.

3. Asymmetric PDI-Based Nonfullerene SMAs

Owing to the low-cost synthesis, high electron mobility, facile functionalization and excellent photo/thermal stability, perylene diimide (PDI) derivatives have received considerable research interests.[18,47,52,53] Due to the large planar π-conjugated system, PDI derivatives generally have a strong aggregation tendency, thus leading to oversized aggregates in their blend film, which is unfavorable for efficient exciton diffusion and separation. To circumvent this problem, several effective strategies have been adopted to reduce the aggregation of the related PDI derivatives, and numerous highly efficient symmetric PDI-based nonfullerene SMAs[15–17] along with a few asymmetric PDI-based nonfullerene SMAs[54,55] have been reported. Among various strategies, constructing PDI dimers through a space unit has been demonstrated as an effective method to design efficient PDI-based nonfullerene SMAs. Nevertheless, these kinds of twisted PDI dimers may affect the coplanarity, which is detrimental to charge transport. Further fusing PDI dimer with a space unit or an aromatic heterocycle may be a promising way to enhance charge transport while maintaining adequate twisting structure for exciton dissociation. For example, when an asymmetric 6-(thiophen-2-yl)-benzo[b]thiophene (T-BTh) as the space unit was inserted between the two PDI units, Zhou and co-workers[54] synthesized an asymmetric acceptor A101, which was further fused to generate another asymmetric acceptor A102. In comparison with nonfused A101, A102 showed higher LUMO energy level, downshifted highest occupied molecular orbital (HOMO) energy level and extended π-conjugation length. When combined with PBDB-T, the twisted A101 significantly suppressed the π–π stacking of PBDB-T, whereas the fused A102 with relatively more planar structure could keep the effective π–π stacking order of PBDB-T. As a result, an improved PCE of 5.65% was obtained for A102-based OSCs, which was higher than that of A101-based OSCs (3.58%). Zhang and co-workers[55] reported an asymmetric acceptor FPDI-Se by introducing one selenophene heterocycle onto the bay position of fused PDI dimer (FPDI) unit, in which fused PDI dimer was obtained through the fusion of two PDI units with a two-carbon space unit. Compared with symmetric FPDI-2Se in which two selenophene heterocycles were incorporated

Chao Li received his master degree in polymer chemistry and physics from Xiangtan University in 2017. He is currently a Ph.D. student under the supervision of Prof. Yanming Sun at School of Chemistry, Beihang University. His research interests include the design and synthesis of asymmetric nonfullerene small molecule acceptors for organic solar cells.

Yanming Sun received his B.S. degree from Shandong University and Ph.D. degree from the Institute of Chemistry, Chinese Academy of Sciences (ICCAS). From 2007 to 2009, he worked at the University of Manchester as a research assistant. From 2009 to 2013, he joined Prof. Alan J. Heeger's group in the University of California at Santa Barbara as a postdoctoral researcher. In 2013, he joined Beihang University as a professor. In 2018, he was financially supported by the National Science Fund for Distinguished Young Scholars. His research interests focus on organic functional materials and optoelectronic devices.

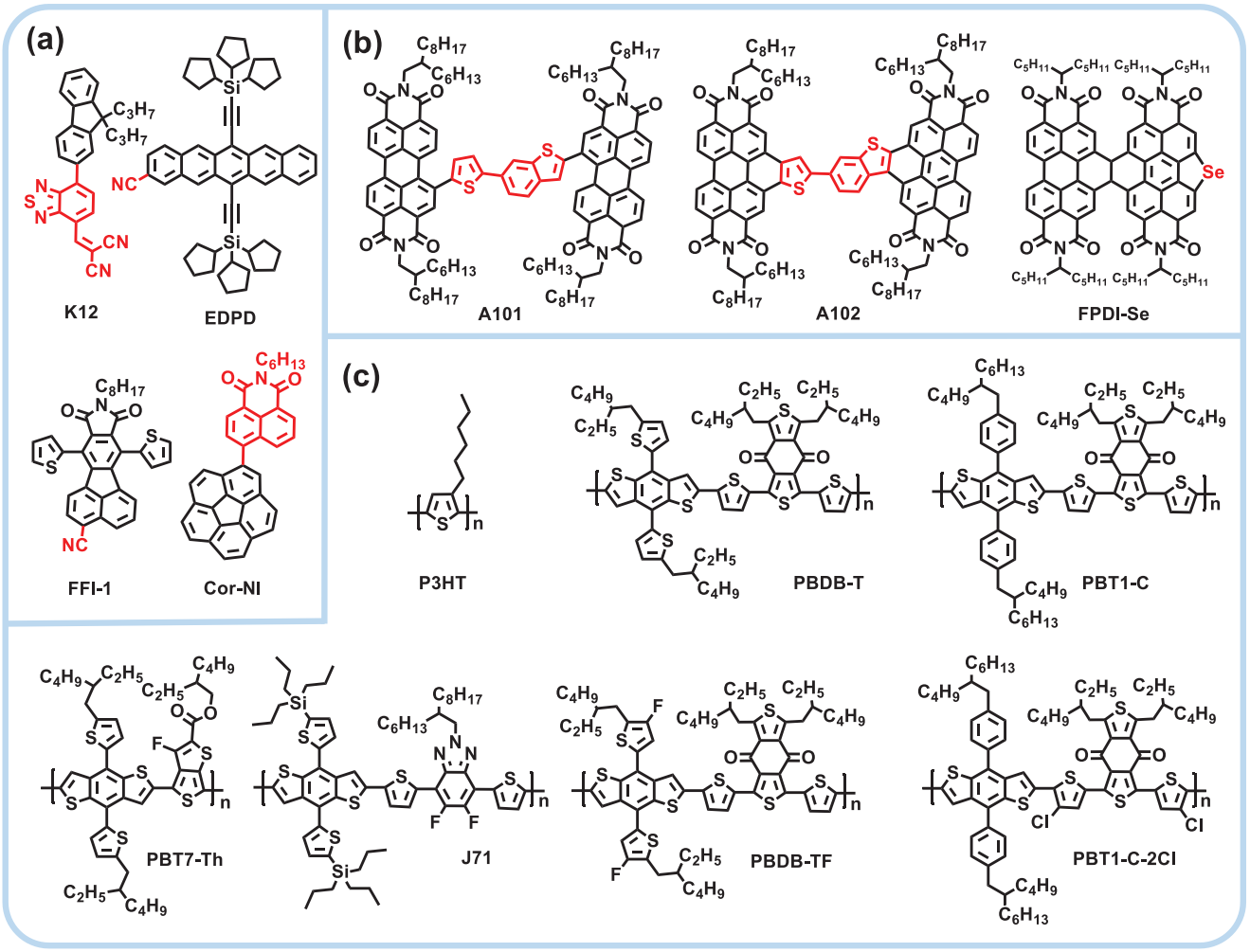

Figure 1. Chemical structures of a) early reports of asymmetric non-fullerene SMAs, b) asymmetric PDI-based nonfullerene SMAs, and c) polymer donors used in this review.

onto the bay positions of FPDI unit, asymmetric FPDI-Se exhibited blue-shifted absorption and higher absorption coefficient in blend film, which enabled PBT7-Th:FPDI-Se OSCs to have a slightly higher J_{sc} than PBT7-Th:FPDI-2Se OSCs. Furthermore, more balanced charge carrier mobility in PBT7-Th:FPDI-Se blend film than that of FPDI-2Se-based blend film endowed PBT7-Th:FPDI-Se OSCs with a significantly higher FF. Finally, a promising PCE of 6.61% was achieved for asymmetric FPDI-Se-based OSCs, whereas the symmetric FPDI-2Se-based OSCs only showed an inferior PCE of 4.45%.

4. Asymmetric A–D–A-Type Nonfullerene SMAs

Since Zhan and co-workers[56] reported ITIC with an A–D–A configuration in 2015, nonfullerene SMAs with the A–D–A configuration have received tremendous research interests and experienced rapid developments.[46,51,57–59] Generally, these A–D–A-type nonfullerene SMAs are composed of three components: central electron-donating core unit (D), outstretched side chain (O), and terminal accepting unit (A). By chemical modification of central D, O, and/or A, the absorption spectra, molecular energy levels, charge transport, and photovoltaic properties of A–D–A-type nonfullerene SMAs could be effectively modulated. When a molecular asymmetry is appeared in D, O, and A, respectively, asymmetric A–D–A-type nonfullerene SMAs can be developed (**Figure 2**).

4.1. Asymmetric A–D–A-Type Nonfullerene SMAs with Asymmetric Cores

Among various central electron-donating core (D) units, indacenodithiophene (IDT or TPT), which integrates thiophene (T), phenylene (P), and thiophene (T) moieties into a single-fused molecular entity, was one of the most widely used building blocks for constructing A–D–A-type nonfullerene SMAs.[60–66] There are several desirable features when IDT was applied into A–D–A- type nonfullerene SMAs.[66,67] The coplanar and rigid ladder-type structures of IDT could extend conjugation, reduce conformational energetic disorder, and facilitate π-electron delocalization, while the side chain attached to the bridging position

Table 1. Optical bandgap, energy levels and photovoltaic parameters for asymmetric non-fullerene SMAs.

NFA	E_g^{opt} [eV]	HOMO/LUMO [eV]	Donor	V_{oc} [V]	J_{sc} [mA cm^{-2}]	FF [%]	PCE [%]	Refs.
K12	–	–6.20/–3.60	P3HT	0.62	2.36	49.8	0.73	[30]
EDPD	1.82	–5.29/–3.50	P3HT	0.84	3.72	41	1.27	[31]
FFI-1	2.60	–6.08/–3.48	P3HT	0.76	4.40	56	1.86	[40]
Cor-NI	3.04	–/–3.24	P3HT	0.82	2.75	46	1.03	[43]
A101	1.98	–5.78/–3.72	PBDB-T	0.85	6.56	64.2	3.58	[54]
A102	2.17	–5.84/–3.65	PBDB-T	0.96	9.66	60.9	5.65	[54]
FPDI-Se	2.23	–6.18/–3.95	PTB7-Th	0.80	14.78	56.1	6.61	[55]
PhITBD	1.72	–5.50/–3.78	PTB7-Th	0.757	14.07	62	6.57	[32]
Me-ITBD	1.69	–5.74/–3.95	PBDB-T	0.89	11.10	58	5.75	[78]
TIDT-BT-R2	1.68	–5.25/–3.65	PTB7-Th	1.04	13.10	63.9	8.7	[80]
TIDT-BT-R6	1.70	–5.28/–3.67	PTB7-Th	1.03	10.3	52.3	5.6	[80]
ITBC	1.59	–5.64/–3.94	PTB7-Th	0.79	13.34	59.49	6.27	[37]
ITBR	1.71	–5.55/–3.71	PTB7-Th	1.02	14.46	51.02	7.49	[37]
ITBRC	1.63	–5.60/–3.82	PTB7-Th	0.91	9.21	51.04	4.26	[37]
ITDI	1.53	–5.89/–4.18	PBDB-T	0.94	14.27	59.72	8.00	[81]
TPTT-IC	1.63	–5.78/–3.95	PBT1-C	0.96	15.6	70	10.5	[33]
A201	1.64	–5.69/–3.93	J71	0.88	13.15	67.15	9.36	[34]
IDT6CN-M	1.65	–5.60/–3.87	PBDB-T	0.91	16.02	76.83	11.20	[35]
TPTT-2F	1.58	–5.75/–4.04	PBT1-C	0.881	15.82	73	10.17	[70]
TPTTT-2F	1.56	–5.69/–4.01	PBT1-C	0.916	17.63	74.5	12.03	[70]
IDT8CN-M	1.58	–5.54/–3.91	PBDB-T	0.920	17.11	78.9	12.43	[90]
MeIC1	1.54	–5.59/–3.89	PBDB-T	0.927	18.32	74.1	12.58	[44]
ITCNTC	1.68	–5.66/–3.92	J71	0.942	14.16	63.8	8.52	[72]
TTPTTT-IC	1.60	–5.64/–3.87	PBT1-C	0.996	12.47	63.7	7.91	[71]
TTPTTT-2F	1.54	–5.67/–4.04	PBT1-C	0.920	16.78	74.6	11.52	[71]
TTPTTT-4F	1.52	–5.69/–4.12	PBT1-C	0.863	19.36	72.1	12.05	[71]
SePT-IN	1.54	–5.77/–4.00	PBT1-C	0.85	16.37	73.3	10.20	[73]
SePTT-2F	1.50	–5.71/–4.00	PBT1-C	0.830	17.51	75	10.90	[74]
SePTTT-2F	1.50	–5.66/–3.97	PBT1-C	0.895	18.02	75.9	12.24	[74]
IDT-OB	1.66	–5.77/–3.87	PBDB-T	0.88	16.18	71.1	10.12	[36]
IDTT-OB	1.59	–5.59/–3.88	PBDB-T	0.91	16.58	74	11.19	[118]
A2	1.61	–5.37/–3.67	J71	0.98	11.63	39.63	4.52	[125]
IDTT-2F-Th	1.55	–5.78/–4.09	PBT1-C-2Cl	0.912	17.82	73.9	12.01	[126]
ITIC-2F	1.56	–5.76/–4.07	PBDB-TF	0.92	17.3	65.7	10.38	[128]
ITIC-3F	1.54	–5.73/–4.12	PBDB-TF	0.89	19.4	66.5	11.44	[128]
a-IT-2OM	1.63	–5.61/–3.92	PBDB-T	0.93	18.11	71.52	12.07	[132]
IT-3F	–	–5.67/–4.09	PBDB-TF	0.90	20.35	75.5	13.83	[38]
ZITI-3F	1.50	–5.64/–3.76	J71	0.90	20.67	71.53	13.15	[134]

of IDT could influence solubility, intermolecular packing, and miscibility with polymer donor.[68] On the basis of IDT, several effective strategies had been adopted to modify IDT structure, which generated a series of symmetric IDT derivatives and asymmetric IDT derivatives[32,33,69–74] (**Figures 3** and **4**):

(i) When a molecular cutting strategy was used to cut one of the bridging carbons in IDT, an asymmetric indenothiophene (IT) derivative[32] (thiophene–indenothiophene) can be developed as an analogue of IDT;

(ii) Core conjugation extension has been adopted to develop not only symmetric IDT derivatives but also asymmetric IDT derivatives. The conventional method is to fuse one thiophene or thieno[3,2-b]thiophene on each side of IDT, which leads to symmetric IDTT[75] and symmetric IBDT,[69] respectively. In contrast, functionalization on only one side of symmetric

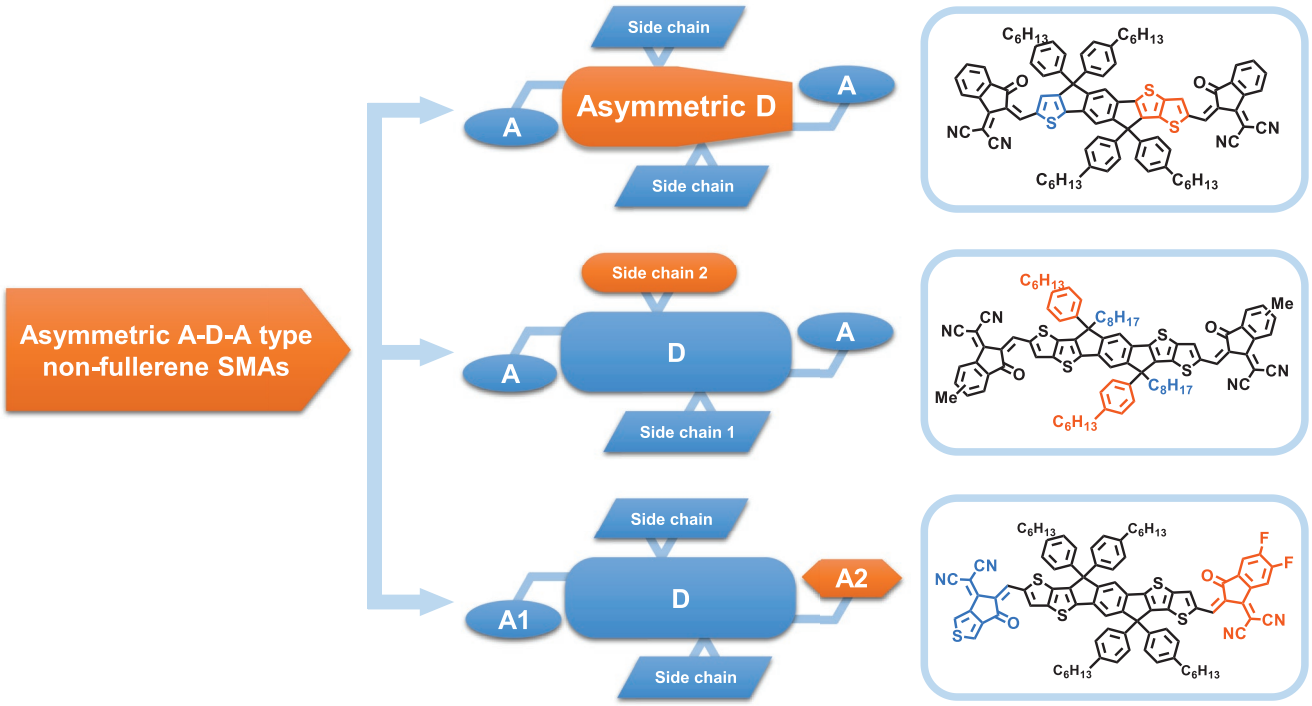

Figure 2. Illustration of three types of asymmetric A–D–A-type nonfullerene SMAs along with representative structures.

core would generate asymmetric extended IDT derivatives. For instance, asymmetric TPTT[33] and TPTTT[70] could be obtained by fusing one thiophene or thieno[3,2-b]thiophene on only one side of IDT, respectively. On the basis of symmetric IDTT, asymmetric TTPTTT[71] could be further developed by fusing one thiophene on only one side of IDTT;

(iii) On the basis of symmetric IDTT, an asymmetric IDTT-S[72] as a novel asymmetric IDT derivative could be further achieved by replacing the thieno[3,2-b]thiophene in symmetric IDTT with thieno[2,3-b]thiophene (T23bT);

(iv) Heteroatom substitution strategy has also shown to be an effective approach to developing IDT derivatives. By substituting one sulfur atom in IDT with a selenium atom, an asymmetric SePT[73] could be designed, while the replacement of two sulfur atom in IDT with two selenium atom could give rise to symmetric IDSe.[76] The asymmetric SePT could be further shifted to asymmetric SePTT[74] and asymmetric SePTTT[74] by rationally extending selephene-containing conjugation length.

Both the asymmetric IT derivative and asymmetric IDT derivatives had been used as asymmetric central cores to construct efficient asymmetric A–D–A-type nonfullerene SMAs.

In 2017, Choi et al.[32] reported asymmetric acceptor PhITBD by utilizing IT derivative as the central core and dicyanovinyl-substituted benzothiadiazole as the terminal accepting unit.

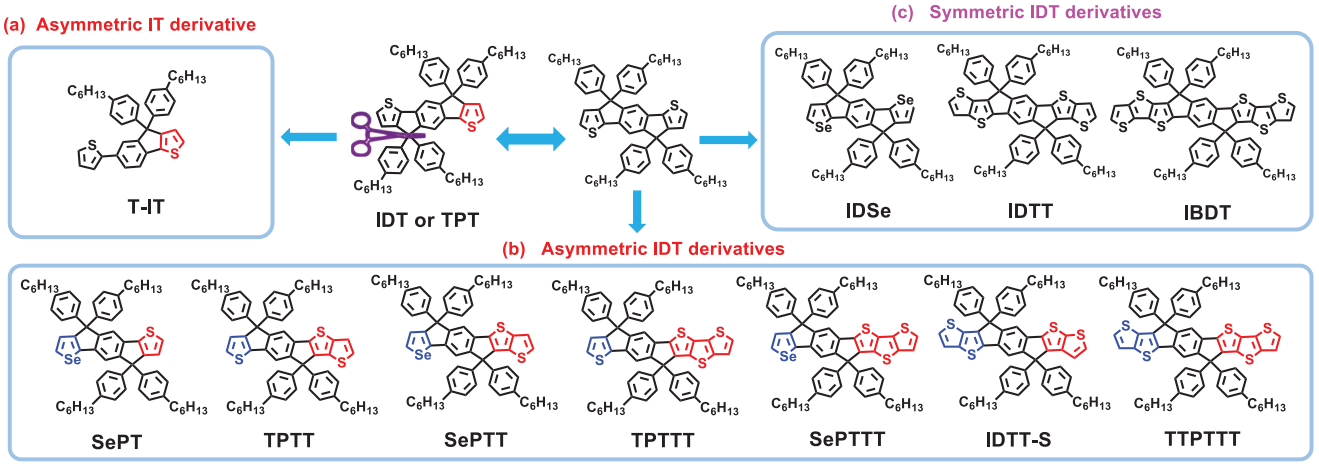

Figure 3. Chemical structures of a) asymmetric IT derivative, b) asymmetric IDT derivatives, and c) symmetric IDT derivatives.

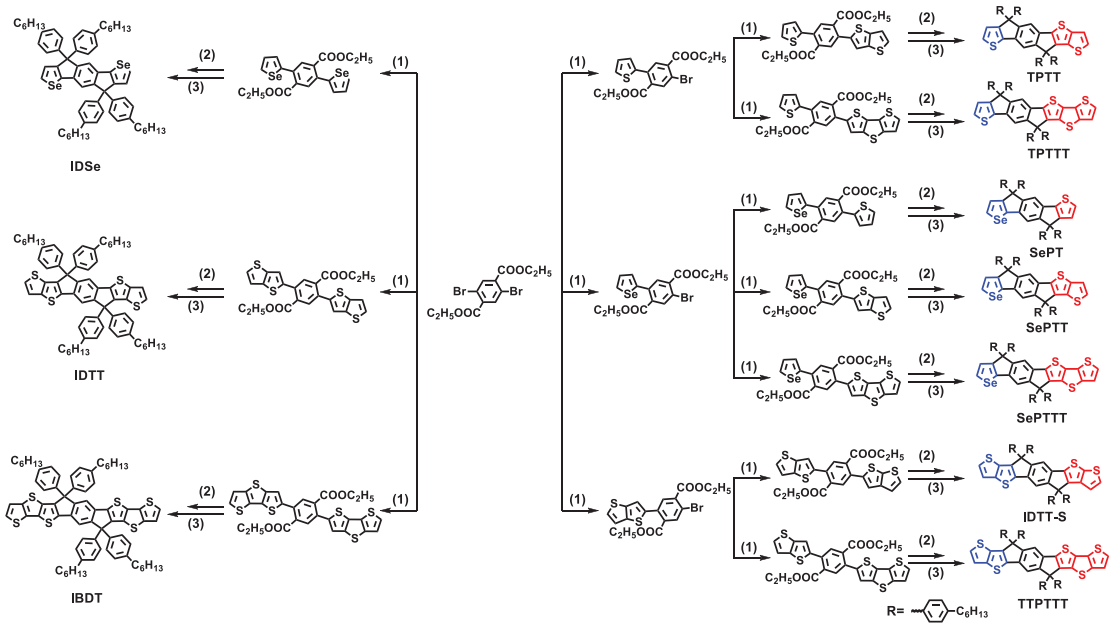

Figure 4. Synthetic routes toward symmetric IDT derivatives and asymmetric IDT derivatives. (1), (2), and (3) represented Still coupling, nucleophilic addition and intramolecular cyclization, respectively.

The twisted structure of asymmetric PhITBD suppressed aggregation behavior and limited compact molecular packing, which may lead to better miscibility with PTB7-Th and thus form smoother surface morphology. Mainly due to more complementary absorption with PTB7-Th, higher molar extinction coefficient of PhITBD, and more balanced charge transport as well as well-defined nanophase segregation in PhITBD-based blend film, the PhITBD-based OSCs (6.57%) showed an enhanced PCE than that of symmetric IDT-2BM[77]-based OSCs (3.97%), which highlights the effectiveness of molecular cutting strategy for designing asymmetric cores and corresponding asymmetric A–D–A-type nonfullerene SMAs. Later, the same group[78] synthesized another asymmetric A–D–A-type nonfullerene SMA named Me-ITBD by introducing a methyl group into the 7-position of indenothiophene unit. The methyl substitution enabled Me-ITBD to have a more twisted structure than PhITBD. They chose PBDB-T[79] as the polymer donor and found Me-ITBD-based blend film exhibited a finer surface morphology and a higher PCE of 5.75% in OSCs than PhITBD-based blend film (1.79%). In 2018, by replacing the dicyanovinyl in PhITBD with rhodanine, Peng and co-workers[80] developed two asymmetric A–D–A-type nonfullerene SMAs, TIDT-BT-R2 and TIDT-BT-R6. TIDT-BT-R2 with shorter side chains showed slightly higher molar extinction coefficient and red-shifted absorption spectrum than TIDT-BT-R6. After blending with PBT7-Th, TIDT-BT-R2-based blend film exhibited more ordered lamellar stacking and stronger π–π stacking than TIDT-BT-R6 based blend film. As a result, the TIDT-BT-R2-based OSCs yielded a higher PCE of 8.7% than that of TIDT-BT-R6-based OSCs (5.6%). By changing the bulky alkylphenyl side chain to flexible alkyl side chain, Zheng and co-workers[37] reported three asymmetric A–D–A-type nonfullerene SMAs, ITBC, ITBR, and ITBRC, to investigate the effect of different terminal accepting units on photovoltaic properties. From ITBR to ITBRC and then to ITBC, red-shifted absorption spectrum, smaller optical bandgap and deeper molecular energy level were obtained, agreeing well with the increased electron-withdrawing ability from 3-ethylrhodanine group (ITBR) to 2-(1,1-dicyanomethylene)-3-ethylrhodanine group (ITBRC) and to dicyanovinyl group (ITBC). As a result, with PBT7-Th as the polymer donor, ITBR-based OSCs gave a highest V_{oc} of 1.02 eV. Moreover, ITBR-based OSCs exhibited a highest J_{sc} of 14.46 mA cm^{-2}. Overall, the ITBR-based OSCs achieved a PCE of 7.49% with a low energy loss of 0.59 eV, higher than the PCE of 4.26% for ITBRC-based OSCs and the PCE of 6.27% for ITBC-based OSCs. With IT derivative and thiophene as the core, the same group[81] reported another asymmetric acceptor ITDI, in which 1,1-dicyanomethylene-3-indanone (IC) was used as the terminal accepting unit. Compared with symmetric CDTDI, asymmetric ITDI showed upshifted LUMO energy level, resulting in a higher V_{oc} in OSCs. Photoluminescence (PL) quenching experimental results showed that the fluorescence emission of PBDB-T was completely quenched by ITDI and vice versa, indicative of efficient exciton efficiency in PBDB-T:ITDI blend film. However, due to the upshifted HOMO energy level of symmetric CDTDI, the fluorescence emission of CDTDI was not completely quenched by PBDB-T. Consequently, the ITDI-based OSCs yielded a PCE of up to 8.00%, substantially higher than that of CDTDI-based OSCs (2.75%).

Following the success of symmetric ITIC with symmetric IDTT core, our group[33] recently reported an asymmetric A–D–A-type nonfullerene SMA TPTT-IC with asymmetric TPTT core, which showed an impressive PCE of 10.5% comparable to ITIC counterpart in OSCs with PBT1-C[82] as the donor polymer. The asymmetric structure of TPTT core, which had a thiophene–phenylene–thieno[3,2-b]thiophene-fused molecular arrangement, enabled the TPTT-IC dimer with three kinds of packing forms by terminal π–π stacking, while there was only

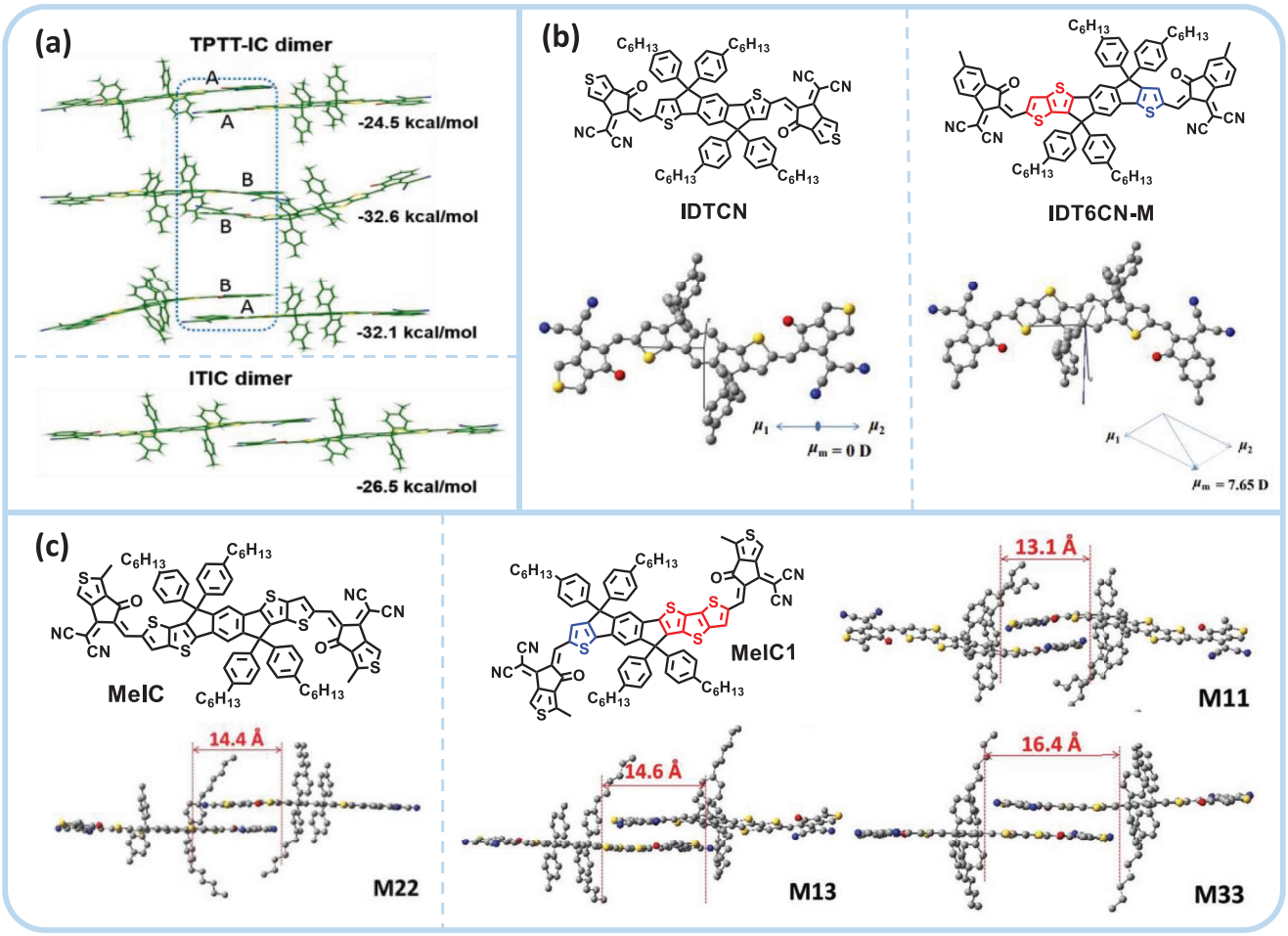

Figure 5. a) Intermolecular binding energies of asymmetric TPTT-IC dimers and symmetric ITIC dimers by DFT calculation. Adapted with permission.[33] Copyright 2018, Royal Society of Chemistry. b) Direction of natural dipole moment of IDTCN (ITCPTC) and IDT6CN-M, and vector addition (μm) of μ_1 and μ_2 produced by one EG and half of asymmetric donor. Adapted with permission.[35] Copyright 2018, Wiley-VCH. c) The structures of two isomers (symmetric MeIC and asymmetric MeIC1) and the geometry configurations of dimer molecules. Adapted with permission.[44] Copyright 2018, Royal Society of Chemistry.

one packing form for the symmetric ITIC dimer (**Figure 5**a). Moreover, this TPTT-IC dimer showed two stronger intermolecular binding energies and two more stable configurations than ITIC dimer. Space charge limited current (SCLC) measurements revealed that TPTT-IC presented higher electron mobility in neat film, higher and more balanced charge carrier transport in blend film as compared with ITIC. In the meantime, Zhou's group[34] and Yang's group[35] also synthesized this asymmetric TPTT core and reported corresponding asymmetric A–D–A-type nonfullerene SMAs. For instance, Zhou and co-workers[34] developed an asymmetric A–D–A type nonfullerene SMA A201 with a same structure of TPTT-IC, which delivered a high PCE of 9.36% in OSCs with J71[83] as the donor polymer. Yang and co-workers[35] reported an asymmetric A–D–A-type nonfullerene SMA IDT6CN-M with a dipole moment of 7.65 Debye (Figure 5b), which was much larger than those of symmetric counterparts (IDTCN and ITCPTC[84]). The large dipole moment in IDT6CN-M could help to strengthen the intermolecular interaction and increase the molecular packing. As a result, the OSCs based on IDT6CN-M afforded an outstanding FF of 76.83% and a PCE of 11.20%, higher than IDTCN-based (FF = 62.48% and PCE = 6.4%) and ITCPTC-based (FF = 72.77% and PCE = 10.74%) OSCs. When 60 wt% symmetric nonfullerene SMA ITCPTC was introduced into the PBDB-T:IDT6CN-M blend, the PCE was improved to be 11.92% in resulting ternary OSCs,[85] which should be ascribed to the improved photon harvesting, good compatibility, and charge transport in ternary active layers.

Core conjugation extension in symmetric A–D–A-type nonfullerene SMAs has demonstrated as an effective approach to improving photovoltaic performance.[86–89] To explore the effect of different asymmetric core conjugation on photovoltaic performance of asymmetric nonfullerene SMAs, our group[70] synthesized one symmetric A–D–A-type nonfullerene SMA TPT-2F and two asymmetric A–D–A-type nonfullerene SMAs (TPTT-2F and TPTTT-2F). From TPT-2F to TPTT-2F and then to TPTTT-2F, successively extending IDT conjugation gave rise to red-shifted absorption spectra, upshifted molecular energy levels, enhanced electron mobilities, and increased intermolecular ordering with improved cofacial π–π stacking (**Figure 6**).

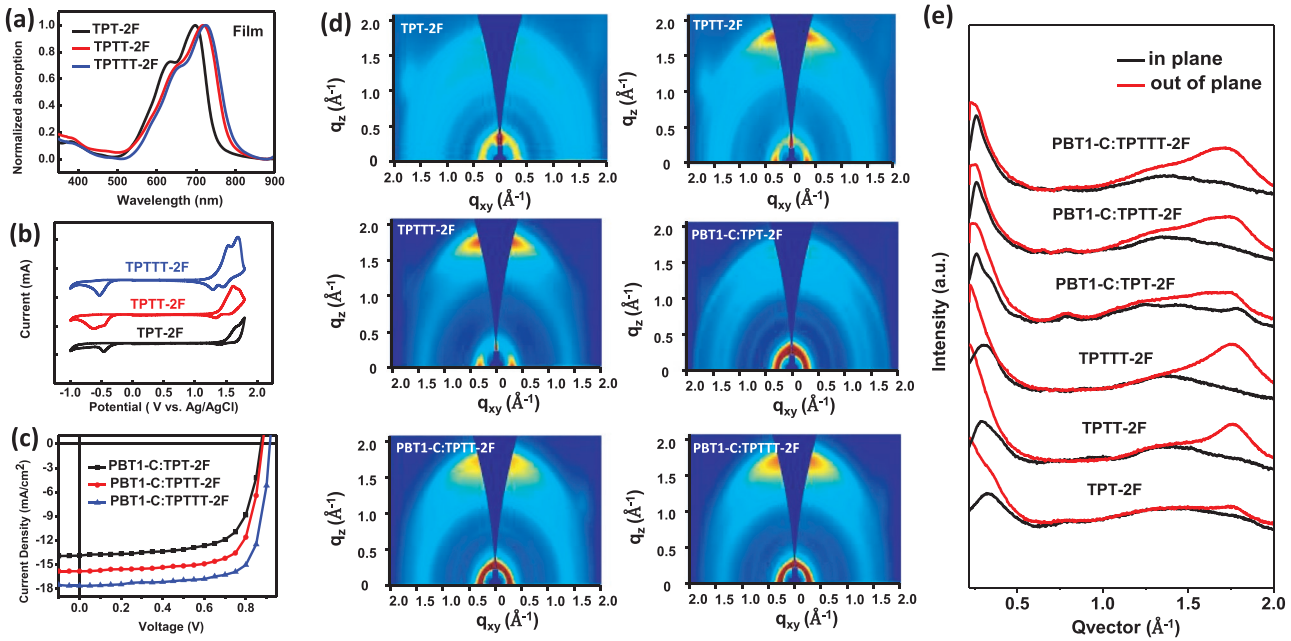

Figure 6. a) Absorption spectra of TPT-2F, TPTT-2F, and TPTTT-2F in thin films. b) Cyclic voltammograms of TPT-2F, TPTT-2F, and TPTTT-2F. c) *J*–*V* curves of OSC devices based on PBT1-C: nonfullerene SMA blend. d) GIWAXS patterns of three nonfullerene SMAs and their corresponding blends. e) In-plane (black lines) and out-of-plane (red lines) line-cut profiles of the GIWAXS results. Adapted with permission.[70] Copyright 2018, Royal Society of Chemistry.

Furthermore, simultaneous enhancements of V_{oc}, $J_{sc,}$ and FF in OSCs were found in the order of TPT-2F < TPTT-2F < TPTTT-2F with PBT1-C as the polymer donor. Consequently, the TPTTT-2F-based OSCs achieved a best PCE of 12.03%, higher than those of OSCs based on TPT-2F (8.33%) and TPTT-2F (10.17%), respectively. Yang and co-workers[90] reported an asymmetric A–D–A-type nonfullerene SMA IDT8CN-M. Besides red-shifting absorption, elevating HOMO energy level and improving electron transport, extending asymmetric core conjugation from IDT6CN-M to IDT8CN-M also enhanced absorption coefficient and increased crystallization propensity. With PBDB-T as the polymer donor, the IDT8CN-M-based OSCs afforded a remarkable PCE of 12.43% and a record FF of 78.9%, which were higher than those of IDT6CN-M-based OSCs (PCE = 11.23% and FF = 76.1%).

Core isomerization has been applied into symmetric A–D–A-type nonfullerene SMAs and proved to have a significant influence on electronic structure, charge transport, and photovoltaic properties.[91,92] In order to investigate the effect of core isomerization on photovoltaic performance of asymmetric A–D–A-type nonfullerene SMA, Yang and co-workers[44] synthesized an asymmetric A–D–A-type nonfullerene SMA MeIC1 with asymmetric TPTTT core, which was an isomer of symmetric MeIC[93] with symmetric IDTT core. Density functional theory (DFT) calculations revealed that asymmetric MeIC1 exhibited three possible packing modes (Figure 5c), slightly higher LUMO energy level, slightly enlarged optical bandgap, and stronger intermolecular bonding energies in comparison with symmetric MeIC counterpart. Asymmetric MeIC1 presented an almost same absorption spectrum as symmetric MeIC in thin films, but a stronger molar absorption coefficient (2.27×10^{-5} M^{-1} cm^{-1}) in chloroform solution, a higher LUMO energy level (−3.89 eV), an enhanced electron mobility (2.38×10^{-3} cm^2 V^{-1} s^{-1}) and an increased π–π stacking than symmetric MeIC (2.09×10^{-5} M^{-1} cm^{-1}, −3.94 eV and 2.03×10^{-3} cm^2 V^{-1} s^{-1}) (**Figure 7**). As a result, the OSCs based on MeIC1 exhibited an outstanding PCE of 12.58% with a V_{oc} of 0.927 V, a J_{sc} of 18.32 mA cm^{-2} and a FF of 74.1%, while symmetric isomer MeIC-based OSCs only delivered a relatively lower PCE of 12.03% with a V_{oc} of 0.896 V, a J_{sc} of 18.07 mA cm^{-2} and an FF of 74.3%. When 50 wt% MeIC1 was added in PBDB-T:INPIC-4F[94] blend, the corresponding ternary OSCs yielded an outstanding PCE of 13.73%,[95] which was mainly due to the simultaneously optimized photo harvesting and favorable film morphology in their ternary active layers. On the basis of asymmetric IDTT-S core, the same group[72] reported an asymmetric A–D–A-type nonfullerene SMA ITCNTC as an isomer of symmetric ITCPTC (**Figure 8**). It was found that asymmetric ITCNTC presented promising characteristics, such as higher LUMO energy level, higher electron mobility, tighter molecular packing, and stronger crystallinity. However, this ITCNTC showed a blue-shifted absorption spectrum, because of the weaker electron-donating capability of asymmetric IDTT-S than that symmetric IDTT, and oversized phase separation in its blend film. In combination with polymer donor J71, the asymmetric ITCNTC-based OSCs delivered a higher V_{oc} of 0.942 V and a significantly lower PCE of 8.52% than the symmetric ITCPTC-based OSCs (0.896 V and 11.63%).[93]

The incorporation of electron-withdrawing fluorine atom into IC end-capping group was beneficial for enhancing electron-deficient nature, charge transporting capability, and ICT effect, which has become an effective approach to design efficient symmetric A–D–A-type nonfullerene SMAs.[69,94] In order to investigate the influence of fluorinated IC group on photovoltaic performance of asymmetric A–D–A-type nonfullerene SMAs, our group[71] reported three asymmetric A–D–A-type nonfullerene SMAs

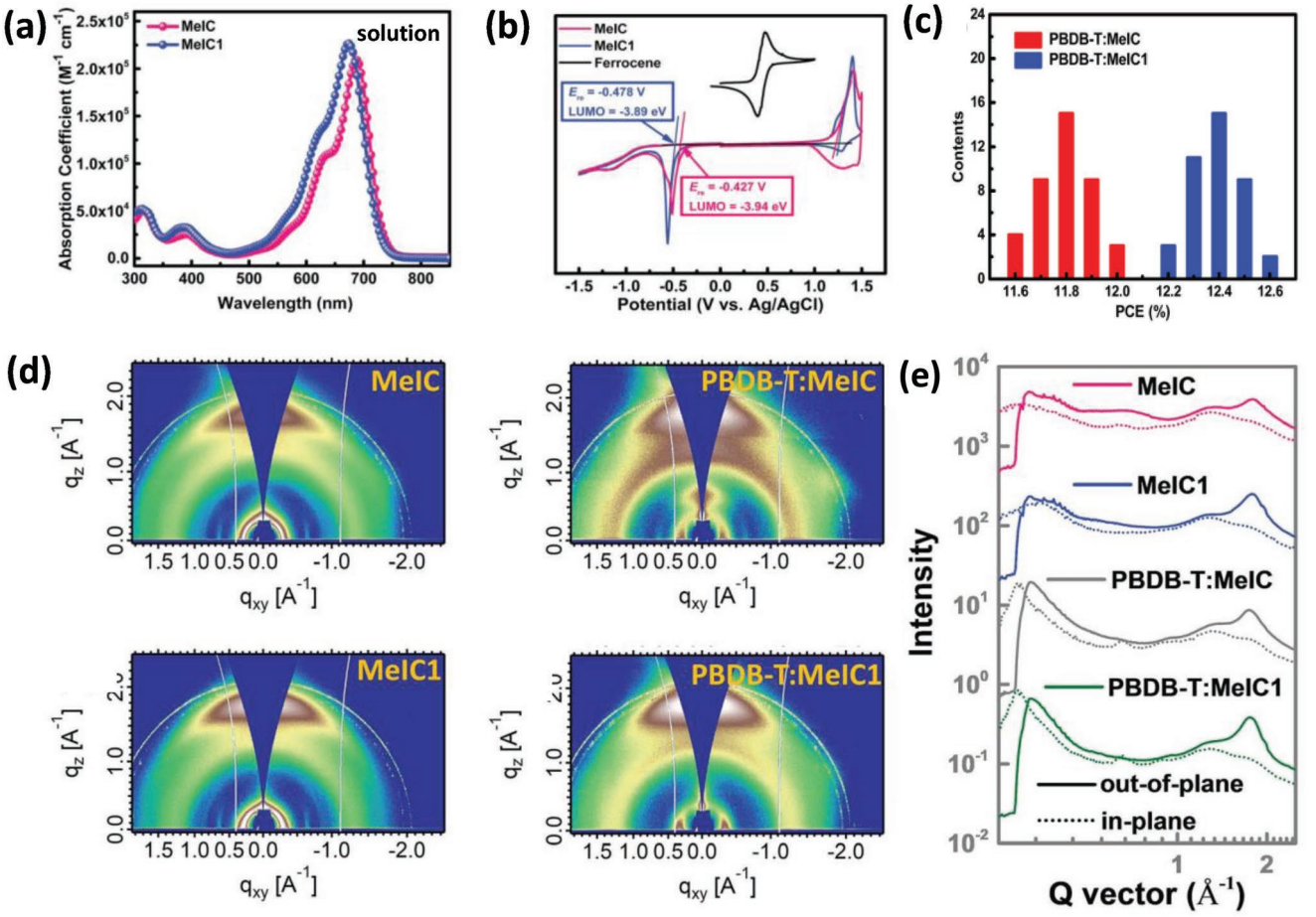

Figure 7. a) Molecular absorption coefficient spectra in chloroform solution. b) CV curves and LUMO energy levels. c) PCE distribution histogram. d) GIWAXS patterns of MeIC- and MeIC1-based neat and blend films. e) Out-of-plane and in-plane GIWAXS cutline profiles. Adapted with permission.[44] Copyright 2018, Royal Society of Chemistry.

(TTPTTT-IC, TTPTTT-2F, and TTPTTT-4F) with asymmetric TTPTTT core. From TTPTTT-IC to TTPTTT-2F and then to TTPTTT-4F, the increase of fluorine atom gave rise to red-shifted light absorption, downshifted molecular energy level, enhanced ICT effect, improved electron mobility and stronger cofacial intermolecular packing. The OSCs based on fluorinated nonfullerene SMAs (TTPTTT-2F and TTPTTT-4F) exhibited lower V_{OC}, substantially higher J_{SC} and FF than nonfluorinated TTPTTT-IC based OSCs. As a result, the OSCs based on TTPTTT-2F and TTPTTT-4F afforded an impressive PCE of 11.52% and 12.05%, respectively, while the nonfluorinated TTPTTT-IC based OSCs only delivered an inferior PCE of 7.91%.

In comparison with thiophene-based A–D–A-type nonfullerene SMAs, selenophene-based A–D–A-type nonfullerene SMAs received relatively less attention.[96–101] In fact, selenophene possessed several merits relative to thiophene. On the one hand, selenophene has more reduced aromaticity and stronger electron-donating capability, which are beneficial to increase quinoidal character, improve backbone planarity, extend conjugation length, and lower optical bandgap.[102–104] On the other hand, selenium atom in selenophene has greater polarizability and larger size than sulfur atom in thiophene, which enabled selenophene to have a tendency to induce intermolecular selenium–selenium interactions or selenium–aromatic interactions.[105–108] Enlightened by these attractive advantages of selenophene over thiophene, our group[73] developed an asymmetric A–D–A-type nonfullerene SMA SePT-IN by substituting one sulfur atom of symmetric TPT-IN[109] with a selenium atom. This heteroatom substitution not only endowed SePT-IN with red-shifted absorption and smaller optical bandgap, but also enabled SePT-IN to have improved electron mobility, elevated HOMO energy level, and interestingly downshifted LUMO energy level as compared to symmetric TPT-IN. Owing to the higher and more balanced charge carrier mobility, more efficient exciton dissociation as well as more efficient charge collection efficiency in asymmetric SePT-IN-based blend film, this asymmetric SePT-IN-based OSCs afforded a decent PCE of 10.20%, higher than that of symmetric TPT-IN-based OSCs (8.91%). The results demonstrated that heteroatom substitution could serve as an effective strategy to design efficient asymmetric A–D–A-type nonfullerene SMAs. Inspired by the success of core conjugation extension,[70] our group[74] reported two selenophene-containing asymmetric A–D–A-type nonfullerene SMAs (SePTT-2F and SePTTT-2F). Interestingly, both two nonfullerene SMAs exhibited similar grazing-incidence wide-angle X-ray scattering (GIWAXS) patterns, optical,

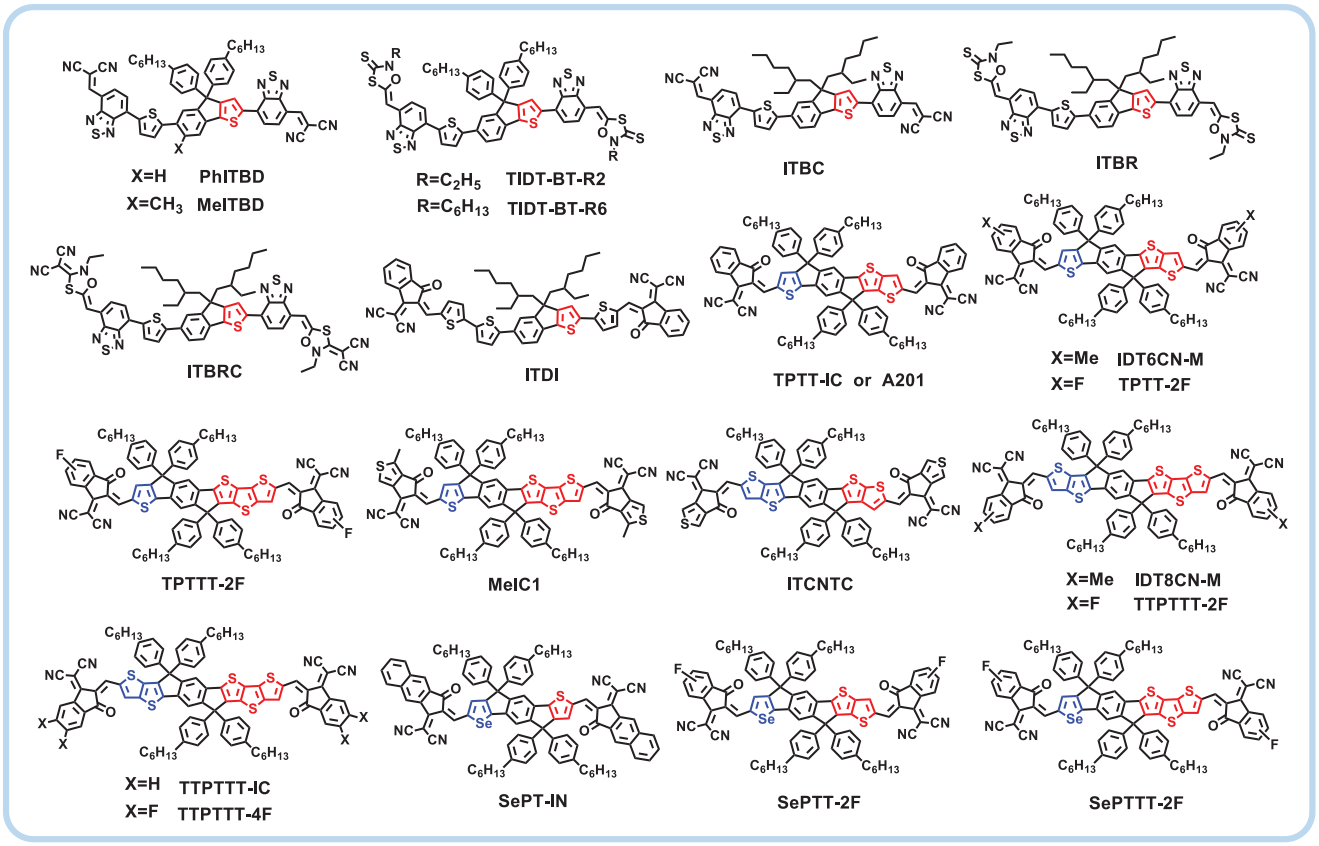

Figure 8. Chemical structures of asymmetric A–D–A-type nonfullerene SMAs with asymmetric cores.

morphological, and photoelectrical characteristics. However, owing to the more extended selenophene-containing backbone conjugation, SePTTT-2F not only presented up-shifted LUMO energy level and increased electron mobility, but also exhibited higher and more balanced charge mobilities in blend film as compared to SePTT-2F. As a result, the SePTTT-2F-based OSCs delivered an impressively high PCE of 12.24% with a V_{oc} of 0.895 V and an FF of 75.9%,while the SePTT-2F based OSCs only achieved an inferior PCE of 10.9% with a V_{oc} of 0.830 V and an FF of 75.0%.

4.2. Asymmetric A–D–A-Type Nonfullerene SMAs with Asymmetric Side Chains

Side chain engineering in A–D–A-type nonfullerene SMAs has a significant effect on solubility, crystallinity, electron mobility, and film morphology.[62,100,110–117] Alkylphenyl side chains attached on the bridging carbons of core could not only help prevent the resulting SMA from forming H-aggregates, thereby forming small phase separation in the blend film, but also make the resulting SMA suffer from large π–π staking distance and low electron mobility. The replacement of alkylphenyl side chains with alkyl side chains could potentially enhance electron mobility and crystallinity of resulting SMAs, which may give rise to forming large domain size in the blend film.[110] Therefore, integration of alkylphenyl and alkyl side chains substituted on symmetric core may be a promising method to simultaneously obtain high electron mobility and avoid undesirably large phase separation. In 2017, Bo and co-workers[36] synthesized an asymmetric A–D–A-type nonfullerene SMA IDT-OB by integrating both alkylphenyl and alkyl side chains substituted on IDT core (**Figure 9**). This asymmetric IDT-OB had several stereoisomers and exhibited a reduced crystallinity without sacrificing close contact in film. After pairing with the PBDB-T, high and balanced charge mobility as well as favorable phase separation was found in the IDT-OB-based blend film (**Figure 10**). As for the blend film based on symmetric IDT-2O with alkyl side chains, stronger crystallinity and larger domain size were found, while the blend film based on symmetric IDT-2B with alkylaryl side chains exhibited lower electron mobility. When IDT-OB was used in OSCs, a promising PCE of 10.12% was obtained. Nevertheless, the IDT-2O-based and IDT-2B-based OSCs only demonstrated a PCE of 9.68% and 6.42%, respectively. Most excitingly, this asymmetric IDT-OB-based OSCs could still maintain a high PCE of 9.17% when the thickness was increased to 210 nm, which represented the highest PCE value for the as-cast thick-film nonfullerene OSCs at that time. By changing the IDT in IDT-OB to the more extended IDTT core, the same group[118] reported another asymmetric A–D–A-type nonfullerene SMA IDTT-OB. In comparison with the asymmetric IDT-OB, this asymmetric IDTT-OB showed increased light-harvesting ability, enhanced crystallinity, and better phased separation morphology when blended with PBDB-T. The maximum PCE of IDTT-OB-based OSCs (11.19%) was higher than that of IDT-OB-based OSCs (10.12%), which

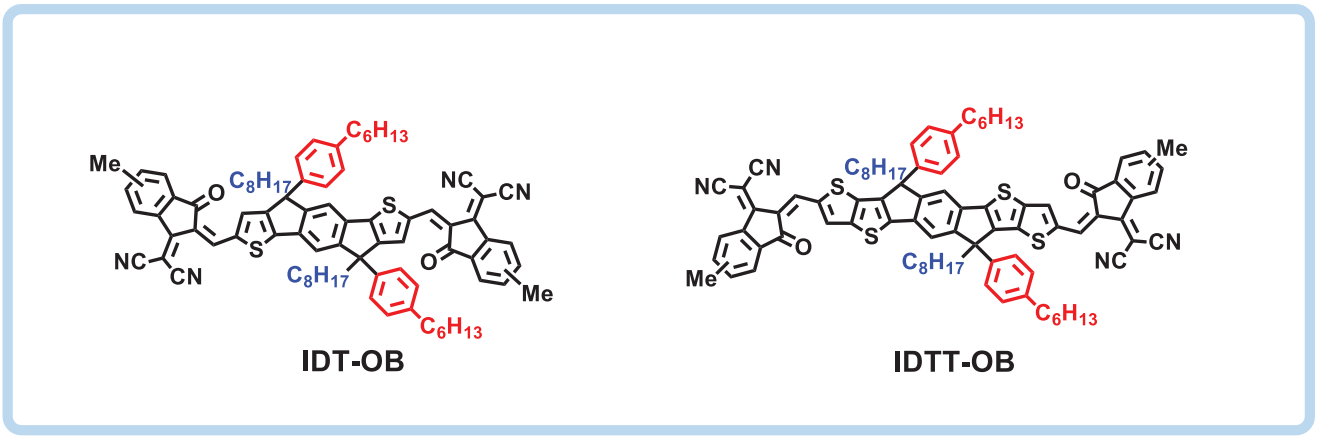

Figure 9. Chemical structures of asymmetric A–D–A-type nonfullerene SMAs with asymmetric side chains.

was ascribed to the concurrent enhancement of V_{oc}, $J_{sc,}$ and FF relative to those of IDT-OB-based OSCs. Moreover, when the active layer thickness was increased to 250 nm, IDTT-OB-based OSCs could still maintain an average PCE of 10.20%, which exemplified the potential of utilizing asymmetric A–D–A-type nonfullerene SMAs to fabricate high-performance thick-film OSCs.

4.3. Asymmetric A–D–A-Type Nonfullerene SMAs with Asymmetric Terminal Groups

In addition to chemical modification of central cores and side chains, terminal group engineering plays an essential role in determining electron mobility, LUMO energy level and bandgap of resultant A–D–A-type nonfullerene SMAs.[119–124] Generally, on the basis of symmetric core, most of A–D–A-type nonfullerene SMAs have two same terminal groups at both ends. When two different terminal groups were introduced at both ends of symmetric core, asymmetric A–D–A-type nonfullerene SMAs with asymmetric terminal groups could be synthesized and developed. For example, Yang et al.[125] reported an asymmetric A–D–A-type nonfullerene SMA A2 by introducing C_{60}-fullerene and IC group as two terminal accepting units (**Figure 11**), which showed good miscibility with J71 and achieved a PCE of 4.52% in OSCs. It was found that A2 showed absorption in the high-energy region (300–500 nm) and low-energy region (500–800 nm) in the thin film, which

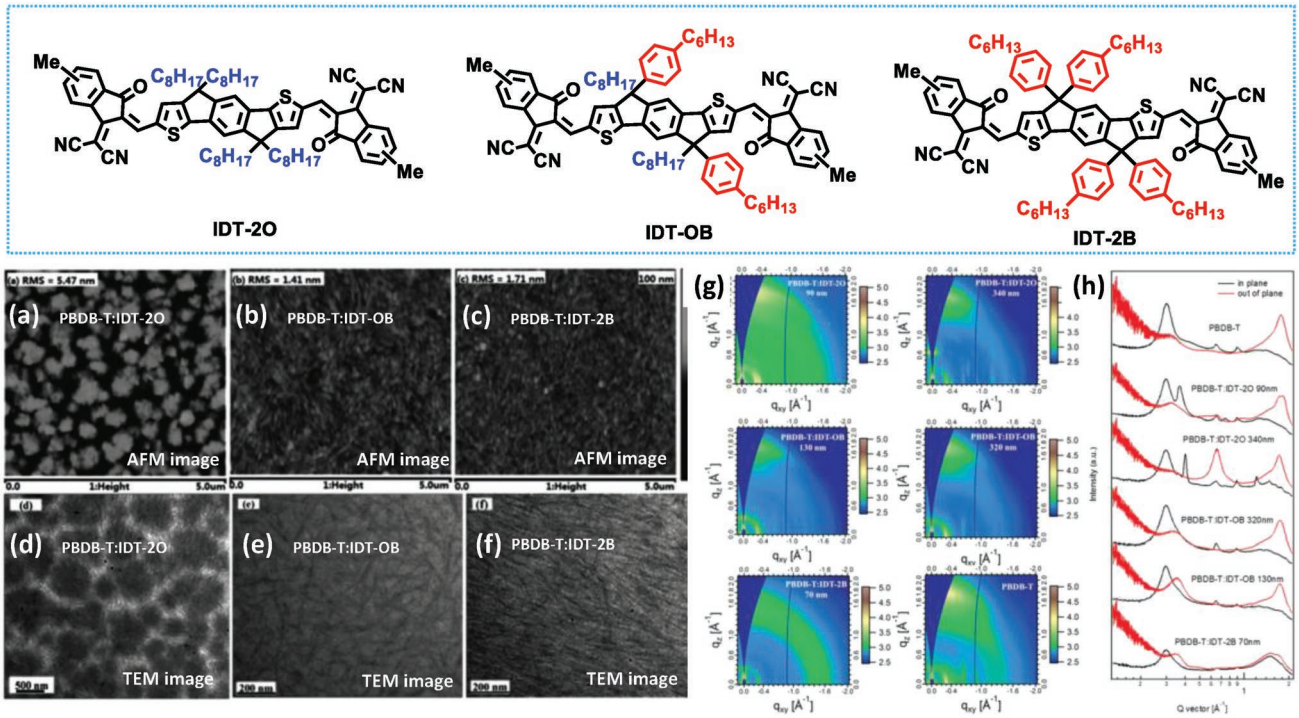

Figure 10. a–c) AFM images of blend films. d–f) TEM images of blend films. g) 2D GIWAXS scattering patterns and line profiles h) of PBDB-T:IDT-2O/OB/2B blend films with different thickness of active layers. Adapted with permission.[36] Copyright 2017, Wiley-VCH.

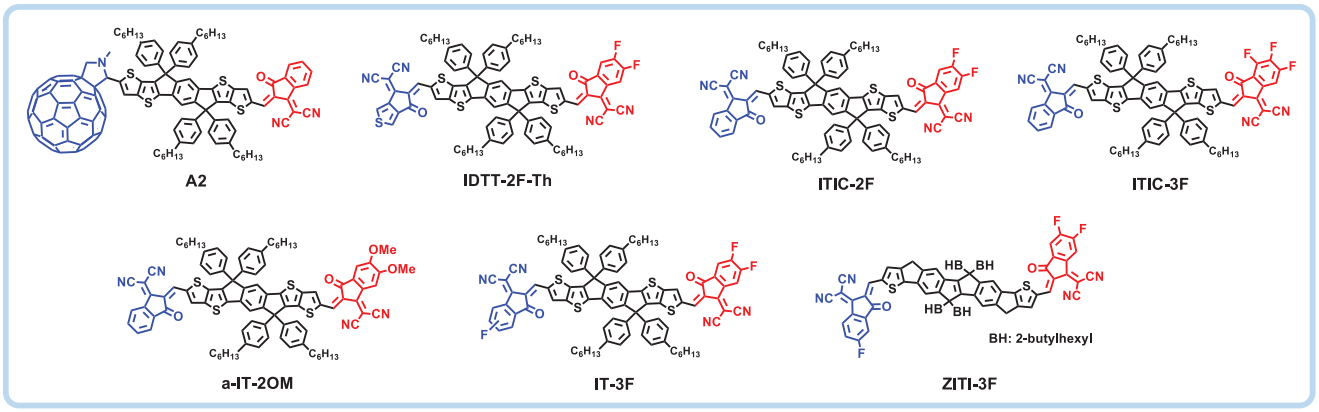

Figure 11. Chemical structures of asymmetric A–D–A-type nonfullerene SMAs with asymmetric terminal groups.

corresponded to fullerene absorption and the absorption from intramolecular interactions between IDTT and IC, respectively. Just recently, our group[126] synthesized an asymmetric A–D–A-type nonfullerene SMA IDTT-F2-Th by replacing one thiophene-fused end-capping group in ITCPTC with a difluorinated IC group. The more stronger electron deficient nature of difluorinated IC group than thiophene-fused end-capping group provided IDTT-2F-Th with a lower lying LUMO energy level and broader optical absorption than ITCPTC, leading to a smaller V_{oc} but a larger J_{sc} in OSCs with PBT1- C-2Cl[127] as the polymer donor (**Figure 12**). IDTT-2F-Th showed a reduced crystallinity in neat film, but more balanced charge transport in blend film when compared with ITCPTC, which was consistent with the higher FF in IDTT-2F-Th-based OSCs. As a result, an overall PCE of 12.01% was obtained for IDTT-2F-Th-based OSCs, which was higher than ITCPTC-based OSCs (10.31%). When one IC group in symmetric ITIC was replaced by a difluorinated IC group[69] or trifluorinated IC group, two asymmetric A–D–A-type nonfullerene SMAs, namely ITIC-2F and ITIC-3F, were synthesized and reported by Marks and co-workers.[128] Due to the asymmetric structures of ITIC-2F and ITIC-3F, an improved molecular ordering and electron

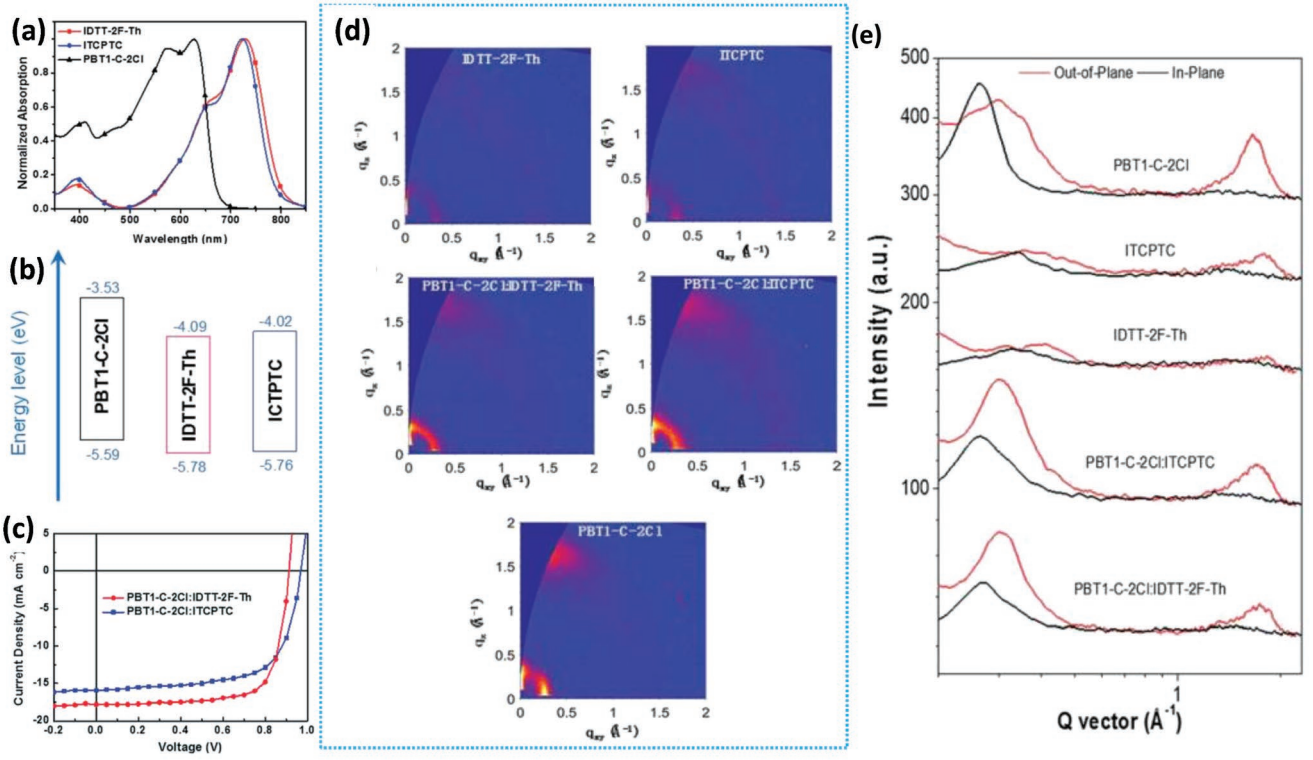

Figure 12. a) Absorption spectra of PBT1-C-2Cl, IDTT-2F-Th, and ITCPTC in thin films. b) Energy-level diagram of PBT1-C-2Cl, IDTT-2F-Th, and ITCPTC. c) *J–V* curves of PBT1-C-2Cl:IDTT-2F-Th and PBT1-C-2Cl:ITCPTC OSC devices. d) GIWAXS patterns of PBT1-C-2Cl, IDTT-2F-Th, and ITCPTC and their corresponding blends. e) In-plane (black lines) and out-of-plane (red lines) line-cut profiles of the GIWAXS results. Adapted with permission.[126] Copyright 2019, Royal Society of Chemistry.

transport in informative ways might be achieved for these two asymmetric nonfullerene SMAs as compared to symmetric nonfullerene SMA counterparts.[129,130] When PBDB-TF[131] was used as the polymer donor, OSCs based on ITIC-2F and ITIC-3F achieved a PCE of 10.38% and 11.44%, respectively, while OSCs based on symmetric ITIC, symmetric IT-4F and symmetric ITIC-6F delivered a PCE of 8.72%, 11.39%, and 11.89%, respectively. In another report, Bo and co-workers[132] synthesized an asymmetric A–D–A-type nonfullerene SMA a-IT-2OM by changing one IC group in symmetric ITIC to a dimethoxy-substituted IC group. Owing to the electron-donating nature of methoxy group, methoxy substitution provided a-IT-2OM with blue-shifted absorption spectrum and upshifted LUMO energy level as compared to ITIC. The OSCs based on a-IT-2OM yielded a promising PCE of 12.07% with PBDB-T as the polymer donor. When active layer thickness was increased to 200 nm, a high PCE over 11% for a-IT-2OM-based OSCs could still be maintained. Hou and co-workers[38] reported an asymmetric A–D–A-type nonfullerene SMA IT-3F through the incorporation of monofluorinated IC and difluorinated IC groups as two different terminal accepting units. SCLC measurements illustrated that asymmetric IT-3F showed an electron mobility of 1.03×10^{-4} cm^2 V^{-1} s^{-1}, which was higher than those of symmetric IT-2F (8.42×10^{-5} cm^2 V^{-1} s^{-1}) and symmetric IT-4F (9.12×10^{-5} cm^2 V^{-1} s^{-1}). The OSCs based on IT-3F yielded an excellent PCE of 13.83% with PBDB-TF as the polymer donor, which was higher than those of IT-2F-based (12.65%) and IT-4F-based (13.62%) OSCs. By replacing the symmetric IDTT core in IT-3F with symmetric dithienocyclopentaindenoindene[133] (FR_{II}) core, Zhu and co-workers[134] rationally synthesized an asymmetric A–D–A-type nonfullerene SMA ZITI-3F. The J71:ZITI-3F devices yielded an outstanding PCE of 13.15%, which was comparable to that of symmetric ZITI-4F-based OSCs (13.18%). The PCE was further promoted to be 13.85% in J71:ZITI-3F:ZITI-4F devices, which was mainly due to the synergistic effect of more broadened absorption, balanced charge transport property, and improved material crystallinity in their ternary blend.

5. Conclusion and Outlook

Among various kinds of asymmetric nonfullerene SMAs, asymmetric A–D–A-type nonfullerene SMAs have become the most widely investigated SMAs and exhibited excellent photovoltaic performance. Mainly benefiting from the development of asymmetric A–D–A-type nonfullerene SMAs, the OSCs based on polymer donor and asymmetric nonfullerene SMA have made tremendous progress with the PCE increasing from 1.27% in 2010 to ≈14% in 2019. Although these exciting advances have been achieved, the development of asymmetric nonfullerene SMAs has still lagged behind as compared to symmetric nonfullerene SMAs. In order to further boost the development of asymmetric nonfullerene SMAs, the future research directions are proposed as follows:

(i) Developing asymmetric A–D–A-type nonfullerene SMAs with asymmetric cores. 1) In addition to utilizing the existing asymmetric IDT derivatives and further developing novel asymmetric IDT derivatives, other asymmetric multifused-ring aromatic electron-donating building blocks would also act as asymmetric cores to construct asymmetric A–D–A-type nonfullerene SMAs. For example, on the basis of a novel asymmetric eight-fused ladder-type core, Yang and co-workers[135] just recently reported an asymmetric A–D–A-type nonfullerene SMA a-BTTIC, which showed a considerably high PCE of 13.60% in OSCs. 2) Introduction of two different side chains into asymmetric core in asymmetric A–D–A-type nonfullerene SMAs has been barely been investigated, which should deserve more attention. 3) For an asymmetric core comprising bridging units, to form intramolecular noncovalent conformational locks would be attractive to design high-performance asymmetric A–D–A-type nonfullerene SMAs. 4) Symmetric core containing electron-withdrawing groups, such as benzothiadiazole and benzotriazole, have emerged to be a new class of core to design high-performance symmetric A–D–A-type nonfullerene SMAs.[22,136–138] Therefore, incorporating electron-withdrawing groups into asymmetric core may be an effective way to further enhance the photovoltaic performances of asymmetric A–D–A-type nonfullerene SMAs.

(ii) Developing asymmetric A–D–A-type nonfullerene SMAs with asymmetric side chains. Currently, there are only two asymmetric A–D–A-type nonfullerene SMAs with asymmetric side chains, both of which have several stereoisomers in the side chains. Therefore, there is enough room for introducing two different side chains into symmetric core to form asymmetric A–D–A-type nonfullerene SMAs with no side chain stereoisomers.

(iii) Developing asymmetric A–D–A-type nonfullerene SMAs with asymmetric terminal groups. Besides symmetric IDTT and FR_{II} cores, introducing two different terminal groups into other symmetric multifused-ring aromatic core is expected to further enrich and develop asymmetric A–D–A-type nonfullerene SMA with asymmetric terminal groups.

(iv) Optimization of asymmetric nonfullerene SMA-based OSCs. For example, three examples of ternary OSCs based on asymmetric nonfullerene SMA had been already reported, which showed better photovoltaic performance than the corresponding binary OSCs. Besides continuing to use one polymer donor, one symmetric nonfullerene SMA and one asymmetric nonfullerene SMA to fabricate ternary OSCs, utilizing one polymer donor and two asymmetric nonfullerene SMAs, or using two polymer donors and one asymmetric nonfullerene SMA to fabricate ternary OSCs could be also promising strategies to further elevate the photovoltaic performance of the binary OSCs.

In conclusion, asymmetric nonfullerene SMAs may possess stronger intermolecular bonding energy and larger dipole moment than the symmetric nonfullerene SMA counterparts, rendering them a promising class of nonfullerene SMAs for OSCs. We believe that continued development of asymmetric nonfullerene SMAs, together with interface engineering, morphology control, device structure optimization, and working mechanism study, will contribute to the further advance of OSCs.

Acknowledgements

This work was financially supported by the National Natural Science Foundation of China (NSFC) (Grant Nos. 21734001, and 21674007).

Conflict of Interest

The authors declare no conflict of interest.

Keywords

asymmetry, nonfullerene small molecule acceptors, organic solar cells, power conversion efficiencies

Received: March 26, 2019
Revised: April 14, 2019
Published online: May 13, 2019

[1] D. Wöhrle, D. Meissner, *Adv. Mater.* **1991**, *3*, 129.
[2] S. Günes, H. Neugebauer, N. S. Sariciftci, *Chem. Rev.* **2007**, *107*, 1324.
[3] G. Li, R. Zhu, Y. Yang, *Nat. Photonics* **2012**, *6*, 153.
[4] Y. Huang, E. J. Kramer, A. J. Heeger, G. C. Bazan, *Chem. Rev.* **2014**, *114*, 7006.
[5] G. Yu, J. Gao, J. C. Hummelen, F. Wudl, A. J. Heeger, *Science* **1995**, *270*, 1789.
[6] L. Huo, T. Liu, X. Sun, Y. Cai, A. J. Heeger, Y. Sun, *Adv. Mater.* **2015**, *27*, 2938.
[7] L. Huo, T. Liu, B. Fan, Z. Zhao, X. Sun, D. Wei, M. Yu, Y. Liu, Y. Sun, *Adv. Mater.* **2015**, *27*, 6969.
[8] L. Lu, T. Zheng, Q. Wu, A. M. Schneider, D. Zhao, L. Yu, *Chem. Rev.* **2015**, *115*, 12666.
[9] H. Yao, L. Ye, H. Zhang, S. Li, S. Zhang, J. Hou, *Chem. Rev.* **2016**, *116*, 7397.
[10] H. Zhou, L. Yang, W. You, *Macromolecules* **2012**, *45*, 607.
[11] L. Dou, Y. Liu, Z. Hong, G. Li, Y. Yang, *Chem. Rev.* **2015**, *115*, 12633.
[12] Y. Lin, X. Zhan, *Mater. Horiz.* **2014**, *1*, 470.
[13] C. B. Nielsen, S. Holliday, H.-Y. Chen, S. J. Cryer, I. McCulloch, *Acc. Chem. Res.* **2015**, *48*, 2803.
[14] W. Chen, Q. Zhang, *J. Mater. Chem. C* **2017**, *5*, 1275.
[15] C. Yan, S. Barlow, Z. Wang, H. Yan, A. K. Y. Jen, S. R. Marder, X. Zhan, *Nat. Rev. Mater.* **2018**, *3*, 18003.
[16] J. Hou, O. Inganäs, R. H. Friend, F. Gao, *Nat. Mater.* **2018**, *17*, 119.
[17] G. Zhang, J. Zhao, P. C. Y. Chow, K. Jiang, J. Zhang, Z. Zhu, J. Zhang, F. Huang, H. Yan, *Chem. Rev.* **2018**, *118*, 3447.
[18] C. Zhan, X. Zhang, J. Yao, *RSC Adv.* **2015**, *5*, 93002.
[19] S. Li, L. Zhan, F. Liu, J. Ren, M. Shi, C.-Z. Li, T. P. Russell, H. Chen, *Adv. Mater.* **2018**, *30*, 1705208.
[20] W. Peng, G. Zhang, L. Shao, C. Ma, B. Zhang, W. Chi, Q. Peng, W. Zhu, *J. Mater. Chem. A* **2018**, *6*, 24267.
[21] G. Zhang, G. Yang, H. Yan, J.-H. Kim, H. Ade, W. Wu, X. Xu, Y. Duan, Q. Peng, *Adv. Mater.* **2017**, *29*, 1606054.
[22] L. Feng, J. Yuan, Z. Zhang, H. Peng, Z.-G. Zhang, S. Xu, Y. Liu, Y. Li, Y. Zou, *ACS Appl. Mater. Interfaces* **2017**, *9*, 31985.
[23] X. Zhang, D. Zhang, Q. Zhou, R. Wang, J. Zhou, J. Wang, H. Zhou, Y. Zhang, *Nano Energy* **2019**, *56*, 494.
[24] H. Lin, Q. Wang, *J. Energy Chem.* **2018**, *27*, 990.
[25] J. Song, X. Xue, B. Fan, L. Huo, Y. Sun, *Mater. Chem. Front.* **2018**, *2*, 1626.
[26] K. Rundel, S. Maniam, K. Deshmukh, E. Gann, S. K. K. Prasad, J. M. Hodgkiss, S. J. Langford, C. R. McNeill, *J. Mater. Chem. A* **2017**, *5*, 12266.
[27] A. A. F. Eftaiha, J.-P. Sun, I. G. Hill, G. C. Welch, *J. Mater. Chem. A* **2014**, *2*, 1201.
[28] F. Liu, T. Hou, X. Xu, L. Sun, J. Zhou, X. Zhao, S. Zhang, *Macromol. Rapid Commun.* **2018**, *39*, 1700555.
[29] W. Li, H. Yao, H. Zhang, S. Li, J. Hou, *Chem. - Asian J.* **2017**, *12*, 2160.
[30] P. E. Schwenn, K. Gui, A. M. Nardes, K. B. Krueger, K. H. Lee, K. Mutkins, H. Rubinstein-Dunlop, P. E. Shaw, N. Kopidakis, P. L. Burn, P. Meredith, *Adv. Energy Mater.* **2011**, *1*, 73.
[31] Y. Shu, Y.-F. Lim, Z. Li, B. Purushothaman, R. Hallani, J. E. Kim, S. R. Parkin, G. G. Malliaras, J. E. Anthony, *Chem. Sci.* **2011**, *2*, 363.
[32] Y. Un Kim, G. Eun Park, S. Choi, D. Hee Lee, M. Ju Cho, D. H. Choi, *J. Mater. Chem. C* **2017**, *5*, 7182.
[33] C. Li, Y. Xie, B. Fan, G. Han, Y. Yi, Y. Sun, *J. Mater. Chem. C* **2018**, *6*, 4873.
[34] W. Zhai, A. Tang, B. Xiao, X. Wang, F. Chen, E. Zhou, *Sci. Bull.* **2018**, *63*, 845.
[35] W. Gao, M. Zhang, T. Liu, R. Ming, Q. An, K. Wu, D. Xie, Z. Luo, C. Zhong, F. Liu, F. Zhang, H. Yan, C. Yang, *Adv. Mater.* **2018**, *30*, 1800052.
[36] S. Feng, C. E. Zhang, Y. Liu, Z. Bi, Z. Zhang, X. Xu, W. Ma, Z. Bo, *Adv. Mater.* **2017**, *29*, 1703527.
[37] C. Tang, S.-C. Chen, Q. Shang, Q. Zheng, *Sci. China Mater.* **2017**, *60*, 707.
[38] B. Gao, H. Yao, J. Hou, R. Yu, L. Hong, Y. Xu, J. Hou, *J. Mater. Chem. A* **2018**, *6*, 23644.
[39] Y. Fang, A. K. Pandey, A. M. Nardes, N. Kopidakis, P. L. Burn, P. Meredith, *Adv. Energy Mater.* **2013**, *3*, 54.
[40] Y. Zhou, L. Ding, K. Shi, Y.-Z. Dai, N. Ai, J. Wang, J. Pei, *Adv. Mater.* **2012**, *24*, 957.
[41] Y. Zhou, Y.-Z. Dai, Y.-Q. Zheng, X.-Y. Wang, J.-Y. Wang, J. Pei, *Chem. Commun.* **2013**, *49*, 5802.
[42] Y.-Q. Zheng, Y.-Z. Dai, Y. Zhou, J.-Y. Wang, J. Pei, *Chem. Commun.* **2014**, *50*, 1591.
[43] R.-Q. Lu, Y.-Q. Zheng, Y.-N. Zhou, X.-Y. Yan, T. Lei, K. Shi, Y. Zhou, J. Pei, L. Zoppi, K. K. Baldridge, J. S. Siegel, X.-Y. Cao, *J. Mater. Chem. A* **2014**, *2*, 20515.
[44] W. Gao, Q. An, C. Zhong, Z. Luo, R. Ming, M. Zhang, Y. Zou, F. Liu, F. Zhang, C. Yang, *Chem. Sci.* **2018**, *9*, 8142.
[45] S. Li, Z. Zhang, M. Shi, C.-Z. Li, H. Chen, *Phys. Chem. Chem. Phys.* **2017**, *19*, 3440.
[46] Z. Liu, X. Zhang, P. Li, X. Gao, *Sol. Energy* **2018**, *174*, 171.
[47] N. Liang, W. Jiang, J. Hou, Z. Wang, *Mater. Chem. Front.* **2017**, *1*, 1291.
[48] D. He, F. Zhao, L. Jiang, C. Wang, *J. Mater. Chem. A* **2018**, *6*, 8839.
[49] Y. Lin, X. Zhan, *Adv. Energy Mater.* **2015**, *5*, 1501063.
[50] Z.-Q. Jiang, T.-T. Wang, F.-P. Wu, J.-D. Lin, L.-S. Liao, *J. Mater. Chem. A* **2018**, *6*, 17256.
[51] H. Wang, J. Cao, J. Yu, Z. Zhang, R. Geng, L. Yang, W. Tang, *J. Mater. Chem. A* **2019**, *7*, 4313.
[52] F. Fernández-Lázaro, N. Zink-Lorre, Á. Sastre-Santos, *J. Mater. Chem. A* **2016**, *4*, 9336.
[53] Z. Liu, Y. Wu, Q. Zhang, X. Gao, *J. Mater. Chem. A* **2016**, *4*, 17604.
[54] F. Chen, G. Ding, A. Tang, B. Xiao, J. Li, E. Zhou, *J. Mater. Chem. C* **2018**, *6*, 2580.
[55] Y. Yin, J. Song, F. Guo, Y. Sun, L. Zhao, Y. Zhang, *ACS Appl. Energy Mater.* **2018**, *1*, 6577.
[56] Y. Lin, J. Wang, Z.-G. Zhang, H. Bai, Y. Li, D. Zhu, X. Zhan, *Adv. Mater.* **2015**, *27*, 1170.
[57] J. Zhang, H. S. Tan, X. Guo, A. Facchetti, H. Yan, *Nat. Energy* **2018**, *3*, 720.

[58] A. Wadsworth, M. Moser, A. Marks, M. S. Little, N. Gasparini, C. J. Brabec, D. Baran, I. McCulloch, *Chem. Soc. Rev.* **2019**, *48*, 1596.
[59] Z. Zhang, J. Yuan, Q. Wei, Y. Zou, *Front. Chem.* **2018**, *6*, 414.
[60] Y. Lin, Z.-G. Zhang, H. Bai, J. Wang, Y. Yao, Y. Li, D. Zhu, X. Zhan, *Energy Environ. Sci.* **2015**, *8*, 610.
[61] Y. Wu, H. Bai, Z. Wang, P. Cheng, S. Zhu, Y. Wang, W. Ma, X. Zhan, *Energy Environ. Sci.* **2015**, *8*, 3215.
[62] Y. Lin, Q. He, F. Zhao, L. Huo, J. Mai, X. Lu, C.-J. Su, T. Li, J. Wang, J. Zhu, Y. Sun, C. Wang, X. Zhan, *J. Am. Chem. Soc.* **2016**, *138*, 2973.
[63] Y. Liu, Z. Zhang, S. Feng, M. Li, L. Wu, R. Hou, X. Xu, X. Chen, Z. Bo, *J. Am. Chem. Soc.* **2017**, *139*, 3356.
[64] H. Yao, Y. Chen, Y. Qin, R. Yu, Y. Cui, B. Yang, S. Li, K. Zhang, J. Hou, *Adv. Mater.* **2016**, *28*, 8283.
[65] F. Liu, Z. Zhou, C. Zhang, T. Vergote, H. Fan, F. Liu, X. Zhu, *J. Am. Chem. Soc.* **2016**, *138*, 15523.
[66] Y. Li, M. Gu, Z. Pan, B. Zhang, X. Yang, J. Gu, Y. Chen, *J. Mater. Chem. A* **2017**, *5*, 10798.
[67] I. McCulloch, R. S. Ashraf, L. Biniek, H. Bronstein, C. Combe, J. E. Donaghey, D. I. James, C. B. Nielsen, B. C. Schroeder, W. Zhang, *Acc. Chem. Res.* **2012**, *45*, 714.
[68] J.-S. Wu, S.-W. Cheng, Y.-J. Cheng, C.-S. Hsu, *Chem. Soc. Rev.* **2015**, *44*, 1113.
[69] S. Dai, F. Zhao, Q. Zhang, T.-K. Lau, T. Li, K. Liu, Q. Ling, C. Wang, X. Lu, W. You, X. Zhan, *J. Am. Chem. Soc.* **2017**, *139*, 1336.
[70] J. Song, C. Li, L. Ye, C. Koh, Y. Cai, D. Wei, H. Y. Woo, Y. Sun, *J. Mater. Chem. A* **2018**, *6*, 18847.
[71] C. Li, J. Song, L. Ye, C. Koh, K. Weng, H. Fu, Y. Cai, Y. Xie, D. Wei, H. Y. Woo, Y. Sun, *Sol. RRL* **2019**, *3*, 1800246.
[72] Z. Luo, G. Li, K. Wu, Z.-G. Zhang, X. Chen, B. Qiu, L. Xue, Y. Li, C. Yang, *Org. Electron.* **2018**, *62*, 82.
[73] C. Li, J. Song, Y. Cai, G. Han, W. Zheng, Y. Yi, H. S. Ryu, H. Y. Woo, Y. Sun, *J. Energy Chem.* **2020**, *40*, 144.
[74] C. Li, T. Xia, J. Song, H. Fu, H. S. Ryu, K. Weng, L. Ye, H. Y. Woo, Y. Sun, *J. Mater. Chem. A* **2019**, *7*, 1435.
[75] Y.-X. Xu, C.-C. Chueh, H.-L. Yip, F.-Z. Ding, Y.-X. Li, C.-Z. Li, X. Li, W.-C. Chen, A. K.-Y. Jen, *Adv. Mater.* **2012**, *24*, 6356.
[76] H.-H. Chang, C.-E. Tsai, Y.-Y. Lai, W.-W. Liang, S.-L. Hsu, C.-S. Hsu, Y.-J. Cheng, *Macromolecules* **2013**, *46*, 7715.
[77] H. Bai, Y. Wu, Y. Wang, Y. Wu, R. Li, P. Cheng, M. Zhang, J. Wang, W. Ma, X. Zhan, *J. Mater. Chem. A* **2015**, *3*, 20758.
[78] C. H. Jeong, Y. U. Kim, C. G. Park, S. Choi, M. J. Cho, D. H. Choi, *Synth. Met.* **2018**, *246*, 164.
[79] D. Qian, L. Ye, M. Zhang, Y. Liang, L. Li, Y. Huang, X. Guo, S. Zhang, Z. A. Tan, J. Hou, *Macromolecules* **2012**, *45*, 9611.
[80] W. Bai, X. Xu, Q. Li, Y. Xu, Q. Peng, *Small Methods* **2018**, *2*, 1700373.
[81] Z. Kang, S.-C. Chen, Y. Ma, J. Wang, Q. Zheng, *ACS Appl. Mater. Interfaces* **2017**, *9*, 24771.
[82] T. Liu, L. Huo, S. Chandrabose, K. Chen, G. Han, F. Qi, X. Meng, D. Xie, W. Ma, Y. Yi, J. M. Hodgkiss, F. Liu, J. Wang, C. Yang, Y. Sun, *Adv. Mater.* **2018**, *30*, 1707353.
[83] H. Bin, L. Gao, Z.-G. Zhang, Y. Yang, Y. Zhang, C. Zhang, S. Chen, L. Xue, C. Yang, M. Xiao, Y. Li, *Nat. Commun.* **2016**, *7*, 13651.
[84] D. Xie, T. Liu, W. Gao, C. Zhong, L. Huo, Z. Luo, K. Wu, W. Xiong, F. Liu, Y. Sun, C. Yang, *Sol. RRL* **2017**, *1*, 1700044.
[85] M. Zhang, W. Gao, F. Zhang, Y. Mi, W. Wang, Q. An, J. Wang, X. Ma, J. Miao, Z. Hu, X. Liu, J. Zhang, C. Yang, *Energy Environ. Sci.* **2018**, *11*, 841.
[86] Y. Li, X. Liu, F.-P. Wu, Y. Zhou, Z.-Q. Jiang, B. Song, Y. Xia, Z.-G. Zhang, F. Gao, O. Inganäs, Y. Li, L.-S. Liao, *J. Mater. Chem. A* **2016**, *4*, 5890.
[87] J. Zhu, Y. Wu, J. Rech, J. Wang, K. Liu, T. Li, Y. Lin, W. Ma, W. You, X. Zhan, *J. Mater. Chem. C* **2018**, *6*, 66.
[88] J. Zhu, Z. Ke, Q. Zhang, J. Wang, S. Dai, Y. Wu, Y. Xu, Y. Lin, W. Ma, W. You, X. Zhan, *Adv. Mater.* **2018**, *30*, 1704713.
[89] B. Jia, S. Dai, Z. Ke, C. Yan, W. Ma, X. Zhan, *Chem. Mater.* **2018**, *30*, 239.
[90] W. Gao, T. Liu, C. Zhong, G. Zhang, Y. Zhang, R. Ming, L. Zhang, J. Xin, K. Wu, Y. Guo, W. Ma, H. Yan, Y. Liu, C. Yang, *ACS Energy Lett.* **2018**, *3*, 1760.
[91] J. Wang, J. Zhang, Y. Xiao, T. Xiao, R. Zhu, C. Yan, Y. Fu, G. Lu, X. Lu, S. R. Marder, X. Zhan, *J. Am. Chem. Soc.* **2018**, *140*, 9140.
[92] Y. Li, L. Zhong, J.-D. Lin, F.-P. Wu, H.-J. Bin, Z. Zhang, L. Xu, Z.-Q. Jiang, Z.-G. Zhang, F. Liu, T. P. Russell, Y. Li, L.-S. Liao, S. R. Forrest, *Sol. RRL* **2017**, *1*, 1700107.
[93] Z. Luo, H. Bin, T. Liu, Z.-G. Zhang, Y. Yang, C. Zhong, B. Qiu, G. Li, W. Gao, D. Xie, K. Wu, Y. Sun, F. Liu, Y. Li, C. Yang, *Adv. Mater.* **2018**, *30*, 1706124.
[94] J. Sun, X. Ma, Z. Zhang, J. Yu, J. Zhou, X. Yin, L. Yang, R. Geng, R. Zhu, F. Zhang, W. Tang, *Adv. Mater.* **2018**, *30*, 1707150.
[95] X. Ma, W. Gao, J. Yu, Q. An, M. Zhang, Z. Hu, J. Wang, W. Tang, C. Yang, F. Zhang, *Energy Environ. Sci.* **2018**, *11*, 2134.
[96] J.-L. Wang, K.-K. Liu, L. Hong, G.-Y. Ge, C. Zhang, J. Hou, *ACS Energy Lett.* **2018**, *3*, 2967.
[97] Y. Li, L. Zhong, F.-P. Wu, Y. Yuan, H.-J. Bin, Z.-Q. Jiang, Z. Zhang, Z.-G. Zhang, Y. Li, L.-S. Liao, *Energy Environ. Sci.* **2016**, *9*, 3429.
[98] Y. Li, D. Qian, L. Zhong, J.-D. Lin, Z.-Q. Jiang, Z.-G. Zhang, Z. Zhang, Y. Li, L.-S. Liao, F. Zhang, *Nano Energy* **2016**, *27*, 430.
[99] Z. Liang, M. Li, X. Zhang, Q. Wang, Y. Jiang, H. Tian, Y. Geng, *J. Mater. Chem. A* **2018**, *6*, 8059.
[100] W. Gao, Q. An, R. Ming, D. Xie, K. Wu, Z. Luo, Y. Zou, F. Zhang, C. Yang, *Adv. Funct. Mater.* **2017**, *27*, 1702194.
[101] S.-S. Wan, C. Chang, J.-L. Wang, G.-Z. Yuan, Q. Wu, M. Zhang, Y. Li, *Sol. RRL* **2019**, *3*, 1800250.
[102] J. J. Intemann, K. Yao, H.-L. Yip, Y.-X. Xu, Y.-X. Li, P.-W. Liang, F.-Z. Ding, X. Li, A. K. Y. Jen, *Chem. Mater.* **2013**, *25*, 3188.
[103] Z. Fei, Y. Han, E. Gann, T. Hodsden, A. S. R. Chesman, C. R. McNeill, T. D. Anthopoulos, M. Heeney, *J. Am. Chem. Soc.* **2017**, *139*, 8552.
[104] D. Liu, B. Kan, X. Ke, N. Zheng, Z. Xie, D. Lu, Y. Liu, *Adv. Energy Mater.* **2018**, *8*, 1801618.
[105] R. S. Ashraf, I. Meager, M. Nikolka, M. Kirkus, M. Planells, B. C. Schroeder, S. Holliday, M. Hurhangee, C. B. Nielsen, H. Sirringhaus, I. McCulloch, *J. Am. Chem. Soc.* **2015**, *137*, 1314.
[106] F.-Y. Cao, C.-C. Tseng, F.-Y. Lin, Y. Chen, H. Yan, Y.-J. Cheng, *Chem. Mater.* **2017**, *29*, 10045.
[107] A. Patra, M. Bendikov, *J. Mater. Chem.* **2010**, *20*, 422.
[108] Z. Zhao, Z. Yin, H. Chen, L. Zheng, C. Zhu, L. Zhang, S. Tan, H. Wang, Y. Guo, Q. Tang, Y. Liu, *Adv. Mater.* **2017**, *29*, 1602410.
[109] R. Li, G. Liu, M. Xiao, X. Yang, X. Liu, Z. Wang, L. Ying, F. Huang, Y. Cao, *J. Mater. Chem. A* **2017**, *5*, 23926.
[110] Z. Fei, F. D. Eisner, X. Jiao, M. Azzouzi, J. A. Röhr, Y. Han, M. Shahid, A. S. R. Chesman, C. D. Easton, C. R. McNeill, T. D. Anthopoulos, J. Nelson, M. Heeney, *Adv. Mater.* **2018**, *30*, 1705209.
[111] Y. Lin, F. Zhao, Q. He, L. Huo, Y. Wu, T. C. Parker, W. Ma, Y. Sun, C. Wang, D. Zhu, A. J. Heeger, S. R. Marder, X. Zhan, *J. Am. Chem. Soc.* **2016**, *138*, 4955.
[112] T. J. Aldrich, S. M. Swick, F. S. Melkonyan, T. J. Marks, *Chem. Mater.* **2017**, *29*, 10294.
[113] M. Chang, Y. Wang, Y.-Q.-Q. Yi, X. Ke, X. Wan, C. Li, Y. Chen, *J. Mater. Chem. A* **2018**, *6*, 8586.
[114] X. Liu, B. Xie, C. Duan, Z. Wang, B. Fan, K. Zhang, B. Lin, F. J. M. Colberts, W. Ma, R. A. J. Janssen, F. Huang, Y. Cao, *J. Mater. Chem. A* **2018**, *6*, 395.
[115] Y. Yang, Z.-G. Zhang, H. Bin, S. Chen, L. Gao, L. Xue, C. Yang, Y. Li, *J. Am. Chem. Soc.* **2016**, *138*, 15011.

[116] C. e. Zhang, S. Feng, Y. Liu, R. Hou, Z. Zhang, X. Xu, Y. Wu, Z. Bo, *ACS Appl. Mater. Interfaces* **2017**, *9*, 33906.
[117] Z. Zhang, M. Li, Y. Liu, J. Zhang, S. Feng, X. Xu, J. Song, Z. Bo, *J. Mater. Chem. A* **2017**, *5*, 7776.
[118] S. Feng, C. e. Zhang, Z. Bi, Y. Liu, P. Jiang, S. Ming, X. Xu, W. Ma, Z. Bo, *ACS Appl. Mater. Interfaces* **2019**, *11*, 3098.
[119] S. Li, L. Ye, W. Zhao, S. Zhang, S. Mukherjee, H. Ade, J. Hou, *Adv. Mater.* **2016**, *28*, 9423.
[120] S.-L. Chang, F.-Y. Cao, W.-C. Huang, P.-K. Huang, K.-H. Huang, C.-S. Hsu, Y.-J. Cheng, *ACS Energy Lett.* **2018**, *3*, 1722.
[121] R. Li, G. Liu, R. Xie, Z. Wang, X. Yang, K. An, W. Zhong, X.-F. Jiang, L. Ying, F. Huang, Y. Cao, *J. Mater. Chem. C* **2018**, *6*, 7046.
[122] D. Yan, W. Liu, J. Yao, C. Zhan, *Adv. Energy Mater.* **2018**, *8*, 1800204.
[123] H. Feng, N. Qiu, X. Wang, Y. Wang, B. Kan, X. Wan, M. Zhang, A. Xia, C. Li, F. Liu, H. Zhang, Y. Chen, *Chem. Mater.* **2017**, *29*, 7908.
[124] H. Yao, L. Ye, J. Hou, B. Jang, G. Han, Y. Cui, G. M. Su, C. Wang, B. Gao, R. Yu, H. Zhang, Y. Yi, H. Y. Woo, H. Ade, J. Hou, *Adv. Mater.* **2017**, *29*, 1700254.
[125] Y. Zhao, Z. Luo, G. Li, J. Luo, Z.-G. Zhang, Y. Li, C. Yang, *Chem. Commun.* **2018**, *54*, 9801.
[126] L. Ye, Y. Xie, Y. Xiao, J. Song, C. Li, H. Fu, K. Weng, X. Lu, S. Tan, Y. Sun, *J. Mater. Chem. A* **2019**, *7*, 8055.
[127] L. Ye, Y. Xie, K. Weng, H. S. Ryu, C. Li, Y. Cai, H. Fu, D. Wei, H. Y. Woo, S. Tan, Y. Sun, *Nano Energy* **2019**, *58*, 220.
[128] T. J. Aldrich, M. Matta, W. Zhu, S. M. Swick, C. L. Stern, G. C. Schatz, A. Facchetti, F. S. Melkonyan, T. J. Marks, *J. Am. Chem. Soc.* **2019**, *141*, 3274.
[129] J. H. Williams, *Acc. Chem. Res.* **1993**, *26*, 593.
[130] T. Okamoto, K. Nakahara, A. Saeki, S. Seki, J. H. Oh, H. B. Akkerman, Z. Bao, Y. Matsuo, *Chem. Mater.* **2011**, *23*, 1646.
[131] M. Zhang, X. Guo, W. Ma, H. Ade, J. Hou, *Adv. Mater.* **2015**, *27*, 4655.
[132] M. Li, Y. Zhou, J. Zhang, J. Song, Z. Bo, *J. Mater. Chem. A* **2019**, *7*, 8889.
[133] W. Liu, J. Zhang, Z. Zhou, D. Zhang, Y. Zhang, S. Xu, X. Zhu, *Adv. Mater.* **2018**, *30*, 1800403.
[134] J. Zhang, W. Liu, S. Chen, S. Xu, C. Yang, X. Zhu, *J. Mater. Chem. A* **2018**, *6*, 22519.
[135] W. Gao, T. Liu, J. Li, Y. Xiao, G. Zhang, Y. Chen, C. Zhong, X. Lu, H. Yan, C. Yang, *J. Mater. Chem. A* **2019**, *7*, 11053.
[136] J. Yuan, T. Huang, P. Cheng, Y. Zou, H. Zhang, J. L. Yang, S.-Y. Chang, Z. Zhang, W. Huang, R. Wang, D. Meng, F. Gao, Y. Yang, *Nat. Commun.* **2019**, *10*, 570.
[137] J. Yuan, Y. Zhang, L. Zhou, C. Zhang, T.-K. Lau, G. Zhang, X. Lu, H.-L. Yip, S. K. So, S. Beaupré, M. Mainville, P. A. Johnson, M. Leclerc, H. Chen, H. Peng, Y. Li, Y. Zou, *Adv. Mater.* **2019**, *31*, 1807577.
[138] J. Yuan, Y. Zhang, L. Zhou, G. Zhang, H.-L. Yip, T.-K. Lau, X. Lu, C. Zhu, H. Peng, P. A. Johnson, M. Leclerc, Y. Cao, J. Ulanski, Y. Li, Y. Zou, *Joule* **2019**, *3*, 1140.